HHS Public Access

Author manuscript

Neurochem Res. Author manuscript; available in PMC 2018 January 01.

Published in final edited form as:

Neurochem Res. 2017 January ; 42(1): 173–190. doi:10.1007/s11064-016-2103-x.

Comparison of Glutamate Turnover in Nerve Terminals and Brain Tissue during [1,6-$^{13}C_2$]Glucose Metabolism in Anesthetized Rats

Anant B. Patel[1,4], **James C.K. Lai**[3], **Golam I.M. Chowdhury**[2], **Douglas L Rothman**[1], and **Kevin L. Behar**[2]

[1]Department of Diagnostic Radiology and Biomedical Imaging, Magnetic Resonance Research Center, Yale University School of Medicine, New Haven, CT 06520

[2]Department of Psychiatry, Magnetic Resonance Research Center, Yale University School of Medicine, New Haven, CT 06520

[3]Department of Biomedical and Pharmaceutical Sciences, College of Pharmacy, Idaho State University, Pocatello, ID 83209

[4]CSIR-Centre for Cellular and Molecular Biology, Uppal Road, Hyderabad 500007, India

Abstract

The ^{13}C turnover of neurotransmitter amino acids (glutamate, GABA and aspartate) were determined from extracts of forebrain nerve terminals and brain homogenate, and fronto-parietal cortex from anesthetized rats undergoing timed infusions of [1,6-$^{13}C_2$]glucose or [2-^{13}C]acetate. Nerve terminal ^{13}C fractional labeling of glutamate and aspartate was lower than those in whole cortical tissue at all times measured (up to 120 min), suggesting either the presence of a constant dilution flux from an unlabeled substrate or an unlabeled (effectively non-communicating on the measurement timescale) glutamate pool in the nerve terminals. Half times of ^{13}C labeling from [1,6-$^{13}C_2$]glucose, as estimated by least squares exponential fitting to the time course data, were longer for nerve terminals (Glu_{C4}, 21.8 min; $GABA_{C2}$ 21.0 min) compared to cortical tissue (Glu_{C4}, 12.4 min; $GABA_{C2}$, 14.5 min), except for Asp_{C3}, which was similar (26.5 vs. 27.0 min). The slower turnover of glutamate in the nerve terminals (but not GABA) compared to the cortex may reflect selective effects of anesthesia on activity-dependent glucose use, which might be more pronounced in the terminals. The ^{13}C labeling ratio for glutamate-C4 from [2-^{13}C]acetate over that of ^{13}C-glucose was twice as large in nerve terminals compared to cortex, suggesting that astroglial glutamine under the ^{13}C glucose infusion was the likely source of much of the nerve terminal dilution. The net replenishment of most of the nerve terminal amino acid pools occurs directly via trafficking of astroglial glutamine.

*Send correspondence to: Dr. Anant Patel (abpatel@ccmb.res.in) at CSIR-Centre for Cellular and Molecular Biology, Hyderabad 500 007, India; or Dr. Kevin Behar (kevin.behar@yale.edu) at MRRC, PO Box 208043, 300 Cedar Street, New Haven, CT 06520; Tel: (203) 737-4121, Fax: (203) 785-6643.

Disclosures/Conflict of Interest: Dr. Behar discloses ownership of Pfizer common stock and consults for Merck. All authors declare that they have no conflict of interest.

Keywords

Glutamate; GABA; synaptosomes; ^{13}C labeled substrates; Nuclear Magnetic Resonance spectroscopy

Introduction

The physical and functional aspects of brain glutamate compartmentation are well-known and essential features of glutamatergic and GABAergic neurotransmission [1–3]. Glutamate plays multiple roles in CNS function. The major excitatory neurotransmitter and precursor of GABA, glutamate is also the precursor of glutamine formed in astrocytes, which is the major source of new glutamate and GABA synthesis in neurons [3, 4]. Glutamate also plays a fundamental role in glucose and mitochondrial energy metabolism in neurons and astrocytes [5–11].

The development and application of nuclear magnetic resonance spectroscopy and mass spectrometry in conjunction with ^{13}C and ^{15}N labeled substrates have greatly advanced studies of carbon and nitrogen metabolism in cultured cells and neural tissues *in vitro* [12–18] and in animal and human brain *in vivo* [19–30]. Analysis of dynamic time courses of ^{13}C enrichment using metabolic modeling has been used to compute absolute rates of specific pathways (e.g., rates of TCA cycle and neurotransmitter cycling) from analysis of ^{13}C amino acid turnover [23, 31–35]. Considerable effort has gone into validating the overall consistency of these models in terms of mass and isotope (carbon and nitrogen) balance, and the calculated fluxes as compared to independent methods [29]. Less well known, however, is the influence that intracellular compartmentation may have on the kinetics of glutamate labeling from ^{13}C-labeled glucose and other substrates.

The energetics of glutamate and GABA neurotransmission has been studied *in vivo* in conjunction with ^{13}C labeled substrate infusion and ^{13}C NMR spectroscopy both in rats [24, 25, 27, 34, 36–39] and in human subjects [23, 28, 40]. Results of these *in vivo* ^{13}C NMR measurements have established a near 1:1 linear relationship between neurotransmitter cycling (V_{cyc}) and neuronal glucose oxidation ($CMR_{glc(ox)N}$) above isoelectricity [27, 39, 41], indicating that in neurons, the energy supporting glutamatergic neurotransmission is provided mainly by the oxidation of glucose in the tricarboxylic acid (TCA) cycle. This relationship is consistent with calculations of the energetics of specific ion flows associated with glutamatergic neurotransmission [42, 43]. Different molecular-mediated coupling mechanisms have been proposed to explain this relationship [10, 44–49]. The *in vivo* ^{13}C NMR spectroscopic measurements of fluxes reflect whole tissue averages of large populations of neurons and astrocytes. The structure of metabolic models of neuron-astrocyte trafficking used to calculate metabolic fluxes from glutamate, GABA and glutamine ^{13}C turnover treats neural cells as single homogeneous compartments, with no differentiation of presynaptic terminals from postsynaptic dendrites or soma. As recent electrophysiological studies [50, 51] and a revised energy budget [52, 53] show greater energy expenditure associated with dendrites, the potential influence of subcellular compartmentation of neurons on the fluxes estimated by MRS is of substantial interest.

The compartmentation of neurotransmitter glutamate and GABA between metabolic and vesicular pools is well known [1, 2]. Nerve terminals isolated from rodents and incubated with substrates labeled in ^{3}H, ^{14}C or ^{13}C have revealed the complex interplay between mitochondrial, cytoplasmic and vesicular components required for neurotransmitter glutamate and GABA synthesis. These studies have characterized precursors and transporters [54–56] and enzymes expressed in nerve terminal mitochondria and cytoplasm [6, 57–59] necessary for the synthesis and release of glutamate and GABA at the synapse [60]. Nerve terminals studied *in vitro,* however, necessarily reflect conditions far removed from their normal cellular and extracellular physiological environment, neural inputs and astroglial interactions. Recently, we reported that nerve terminals isolated from rodents immediately *after* a timed intravenous infusion of ^{13}C-labeled glucose retain high levels of glutamate and GABA providing a measure of their *in vivo* enrichment at the time of euthanasia. Thus, the ability to isolate presynaptic nerve terminals, the crucial neuronal compartment of glutamate/GABA-glutamine cycling, provides an opportunity to validate and more accurately interpret metabolic fluxes determined in brain tissue *in vivo* using ^{13}C magnetic resonance spectroscopy with multi-compartment metabolic modeling.

In this study, ^{13}C turnover of neurotransmitter glutamate and GABA was investigated in presynaptic nerve terminals isolated from the forebrain of rats infused with [1,6-$^{13}C_2$]glucose and [2-^{13}C]acetate and compared with the corresponding values in forebrain homogenates and cerebral cortex. We find, consistent with prior studies of cerebral cortical tissue, that net replenishment of nerve terminal glutamate and GABA occurs directly via trafficking of astroglial glutamine. In the nerve terminals, the turnover kinetics of glutamate (but not of GABA) was slower compared to the cortex, possibly reflecting selective effects of anesthesia on activity-dependent glucose use, which might be more pronounced in terminals. There is also a higher dilution of glutamate in the nerve terminals, consistent with glutamine trafficking occurring there.

MATERIALS AND METHODS

Animal Preparation

All animal experiments were performed in accordance with the National Institutes of Health Guide for the Care and Use of Laboratory Animals and protocols were approved by the Yale Animal Care and Use Committee. Male Wistar rats (160–180g), were fasted overnight, anesthetized with 2–3% halothane in 30% O_2/67–68%N_2O, tracheotomized, and ventilated. The left femoral artery was cannulated for continuous monitoring of arterial blood pressure and intermittent sampling of blood for the measurement of glucose and gases. The left femoral vein was cannulated for the infusion of [1,6-$^{13}C_2$]glucose or [2-^{13}C]acetate. Body temperature was maintained near 37°C using a heating pad connected to a temperature-regulated circulating water bath. Following surgery, the halothane flow was reduced to ~1% to maintain blood pressure in the normal range.

Infusion of [1,6-$^{13}C_2$]Glucose

[1,6-$^{13}C_2$]Glucose (99 atom %, Cambridge Isotopes, Andover, MA) was infused intravenously for fixed times of 8 min (2.25 mmol·kg^{-1}), 20 min (2.86 mmol·kg^{-1}), 60 min

(4.92 mmol·kg^{-1}) and 120 min (8.00 mmol·kg^{-1}) in rats maintained under halothane anesthesia using an infusion rate schedule [19] that raises plasma glucose rapidly (<1 min) and maintains a nearly constant level and enrichment thereafter. The concentration of the infused ^{13}C-glucose was determined for each animal according to body weight (3.75 mole·L^{-1}·kg^{-1}). Data from animals infused for 8 min (n=6) and 60 min (n=3 of 5) were taken from a previous study [48] in which animals also received a small amount of 2-fluoro-2-deoxyglucose with the [1,6-$^{13}C_2$]glucose. A separate group of rats received an infusion of [2-^{13}C]acetate (0.25 mmol·kg^{-1}·min^{-1}) for 20 min using a rate schedule described previously [24]. At the end of the respective infusions, rats were decapitated and their brains removed for cortical tissue sampling and isolation of nerve terminals.

Isolation of Nerve Terminals

The nerve terminals (NT) were isolated from the forebrain (entire brain excluding cerebellum and olfactory bulb) using the differential and gradient centrifugation method of Lai and Clark [61]. Briefly, rats were decapitated at the appropriate times, brains were quickly removed and the weight recorded using pre-weighed beakers containing ice-cold isolation medium (0.32 M sucrose, 10 mM HEPES, and 1 mM EDTA at pH 7.4). A small quantity (~40 mg) of intact neocortical tissue (fronto-parietal cortex, Ctx) was dissected and frozen for subsequent extraction and analysis. The forebrain tissue was chopped into small pieces using dissection scissors and allowed to settle briefly before decanting the surrounding fluid to remove residual blood. Fresh ice-cold isolation medium was then added to the tissue (10:1 vol/wt) in a large Kontes glass homogenizer, and the tissue was carefully homogenized by several directed passes using the A and B pestles. A fraction (10%) of the resulting homogenate (Hom) was retained and frozen for subsequent extraction and analysis. The remaining homogenate (90%) was centrifuged at 1,300x*g* for 3 min, and supernatants were collected. The resulting pellets were re-suspended in 10 ml of the isolation medium, re-homogenized and then centrifuged at 1300x*g* for 3 min. The supernatants were pooled and centrifuged at 17,000x*g* for 10 min to obtain the crude mitochondrial fraction. The resulting pellet was re-suspended in 15 ml of isolation medium and carefully layered onto a Ficoll gradient (11 mL of 7.5% wt/vol over 11 mL of 10% wt/vol), followed by centrifugation (in a Beckman SW28 rotor, 99,000x*g*, 45 min). The nerve terminals sedimented at the interface between the 7.5% and the 10% Ficoll gradient. They were collected using a transfer pipette, washed twice with NaCl (150 mM) to remove residual sucrose, and pelleted by centrifugation (17,000x*g*, 10 min). The nerve terminals were assumed to be relatively pure based on previous findings of low activity of the astrocytic markers, glutamine synthetase and GFAP, and their characteristic appearance by electron microscopy where the same isolation method was employed [48].

Extraction of Metabolites from Forebrain Nerve Terminals, Forebrain Homogenate and Fronto-Parietal Cortex and Preparation of Supernatants for NMR Spectroscopy

Nerve terminal (NT) pellets were homogenized with ice-cold ethanol (1:6 vol/vol; ethanol 60%: deionized water 40%) in an Eppendorf tube with plastic pestle until no visible pieces remained. [2-^{13}C]glycine (10 mM, 25 μL) was added as an internal concentration reference to correct for potential losses during the extraction procedure. The homogenate was frozen

and thawed three times to ensure complete cell lysis, and clarified by centrifugation (20,000xg).

The frozen forebrain homogenate (Hom) was mixed with ice-cold ethanol (1:6 vol/vol; ethanol 60%: deionized water 40%) in an ice-cold glass homogenizer, frozen and thawed three times to ensure complete cell lysis, and clarified by centrifugation (20,000xg). The supernatant, which contained the relevant amino acids and high levels of sucrose, was applied over an anion exchange column (AG 1-X8) for isolation of the amino acids. Neutral amino acids (GABA and glutamine) and sucrose were eluted using deionized water, whereas glutamate and aspartate were eluted using 2M acetic acid. The glutamate fraction was lyophilized and processed for NMR spectroscopy as described below. Since the neutral fraction (containing GABA and glutamine) contained a very high concentration of sucrose with extensive degree of overlapping NMR signals, GABA and glutamine were not measured in the homogenate (Hom).

The frozen fronto-parietal cortex (40–50 mg) was extracted by pulverizing tissue with 0.1M HCl:MeOH (2:1 vol/wt) in a dry-ice/ethanol bath, then transferred to a wet-ice bath wherein the tissue was homogenized with ice-cold ethanol followed by centrifugation and prepared for NMR as described next.

The supernatants (metabolite fraction) of nerve terminals (NT), homogenates (Hom) and cortex (Ctx) were lyophilized, and re-suspended in 500 μL of a phosphate-buffered (100 mM, pH 7) deuterium oxide (Cambridge Isotopes, Andover, MA) solution containing 3-trimethylsilyl[2,2,3,3-D_4]-propionate (0.25 mM), as chemical shift reference.

NMR Spectroscopy and Analysis of Plasma and Brain Extracts

All NMR spectra were acquired at 11.7 Tesla on a Bruker AVANCE NMR spectrometer (Bruker Instruments, Billerica, MA). Blood plasma was mixed with D_2O and large macromolecules were removed by passage of the samples through a centrifugal filter (10kD cut off, Nanosep, Gelman Laboratory, MN). The percentage ^{13}C enrichment of plasma glucose-C1α was determined from the fully relaxed ^{1}H NMR spectrum by dividing the intensities of the two ^{13}C satellites by the total ($^{12}C+^{13}C$) intensity centered at 5.23 ppm.

Fully relaxed ^{1}H-[^{13}C]-NMR spectra of neural preparations were acquired as described earlier [48, 62]. Metabolite concentrations were determined relative to the added [2-^{13}C]glycine (reference standard) in the ^{13}C difference spectrum. Isotopic ^{13}C enrichment refers to the ratio of metabolite resonance area in the difference spectrum (^{13}C only) to total area in the non-edited spectrum ($^{12}C+^{13}C$), minus 1.1% natural abundance.

Determination of Amino Acid Turnover Parameters

Rate constants (k) of ^{13}C turnover of amino acids were estimated by non-linear least-squares fitting of an exponential function to the time course data using GraphPad Prism software, version 6 (GraphPad Software, Inc., La Jolla, CA). During the fitting both k ($\tau_{1/2} = \ln 2/k$) and steady state ^{13}C labeling were iterated to achieve the best fit of the exponential function to the experimental data.

Determination of Metabolic Fluxes for Cortical Tissue using Metabolic Modeling

Metabolic fluxes were determined by fitting the three-compartment metabolic model (glutamatergic neuron, GABAergic neuron and astroglia) to the time courses of ^{13}C enrichments of Asp_{C3}, $GABA_{C2}$, $GABA_{C3}$, Glu_{C4}, Glu_{C3}, and Gln_{C4} generated *ex vivo* after [1,6-$^{13}C_2$]glucose infusion [24]. The reliability of the flux estimates was improved by using fixed values of the ratios, $V_{cyc(Glu\text{-}Gln)}/V_{TCA(Glu)}$ (0.45) and $V_{cyc(GABA\text{-}Gln)}/V_{TCA(GABA)}$ (0.63) as determined by Patel *et al.* [24]. These values were determined in fronto-parietal cortex of halothane-anesthetized Sprague-Dawley rats for isotopic steady state following an [2-^{13}C]acetate infusion (2 hours) (see Supplement Material in [24] for a derivation of the equations used to calculate the respective V_{cyc}/V_{TCA} ratios). Thus, the ratio values reflect the same conditions of anesthesia and brain region measured in the present study. In brief, mass and ^{13}C isotope flows from [1,6-$^{13}C_2$]glucose into neuronal and astroglial metabolite pools were written as coupled differential equations within the CWave software package. The differential equations were solved numerically using a $1^{st}/2^{nd}$ order Runge-Kutta method, and curves were fitted using the Levenburg-Marquardt algorithm.

Statistics

Parameter estimates are reported as mean ± standard deviation (SD). Statistical significance levels (*P*-values) for comparisons of between-group differences in turnover rate constants (*k*) were estimated from their uncertainty distributions based on 1000 Monte-Carlo simulations of each data set using CWave software. *P*-values were multiplied by 3 to adjust for three comparisons (nerve terminals, homogenate and cortex) and reported as P_{adj}. Statistical significance of between-group differences in ^{13}C enrichment at the different infusion times was assessed by Repeated-Measures One-Way ANOVA and Tukey's post-hoc test using OriginPro 2016 software (OriginLab, Northampton, MA USA). The uncertainties in the absolute fluxes obtained by fitting the metabolic model to the cortical time course data were assessed by Monte-Carlo simulation with 1000 iterations. *P*-values <0.05 were considered statistically significant.

Results

^{13}C Labeling of Amino Acid in Nerve Terminals and Brain Tissue Extracts

Carbon-13 isotopic enrichments in extracts of forebrain nerve terminals, forebrain homogenate and a piece of fronto-parietal cortical tissue were determined from the ^1H-[^{13}C]-NMR spectra. Fig. 1 shows an example of the ^{13}C-labeled methylene spectral region of the extracted nerve terminals and parietal cortex of a single animal following an infusion of [1,6-$^{13}C_2$]glucose for 120 min. Prominent ^{13}C labeling is seen (in order of decreasing intensity) in Glu_{C4}, Glu_{C3}, $GABA_{C2}$, $GABA_{C3}$, and Asp_{C3}. Amino acid labeling patterns in nerve terminals and cortical tissue were qualitatively similar, with exception of Gln_{C4} present in cortical tissue, but absent from the nerve terminals. The relative concentration of GABA to glutamate was considerably higher in the nerve terminal fraction, which could reflect a higher recovery of GABAergic nerve terminals or relatively more synapses in the mid-brain, although autolytic production from glutamate is also a possibility.

Isotopic Turnover of Amino Acids in Nerve Terminals and Tissues

Fig. 2 depicts the time courses of ^{13}C labeling (expressed as percentage ^{13}C enrichment) of Glu_{C4}, Glu_{C3}, $GABA_{C2}$ and Asp_{C3} in forebrain nerve terminals and homogenate (excluding GABA), and fronto-parietal cortex (including Gln_{C4}) from a series of timed infusions of [1,6-$^{13}C_2$]glucose. The ^{13}C enrichment levels in the amino acids rose progressively with time for all measured carbon positions and within the respective preparations in the order $Glu_{C4} > GABA_{C2} > Gln_{C4}$ (cortex) ≈ $Asp_{C3} > Glu_{C3}$ with asymptotic approach to approximately constant (steady-state) values for Glu_{C4}, $GABA_{C2}$ and Gln_{C4}.

The Glu_{C4} enrichment was significantly lower in forebrain nerve terminals compared to homogenate or cortex for all infusion times ($P<0.02$ to $P<0.0001$; Fig. 2, table inset; Supplementary Material, Table S1). There was a trend toward lower Glu_{C4} enrichments in homogenate compared to cortex for early time points, but the difference was significant only for 60 min ($P<0.05$) and for the combined (60+120 min) ($P<0.01$) data. The Glu_{C3} enrichment in nerve terminals was significantly lower than in cortex ($P<0.05$) but not in homogenate for the 8 min time point, while no other time points showed significant differences. In nerve terminals, Asp_{C3} enrichment at 60 min differed significantly from homogenate ($P<0.05$) and cortex ($P<0.01$), although data scatter was particularly high at this time point. The $GABA_{C2}$ enrichments in nerve terminals and cortex were similar for all time points although slightly lower enrichment ($P<0.05$) was seen in the nerve terminals for the combined (60 min plus 120 min) data.

For the nerve terminals, homogenate and cortex the turnover rate constants (and corresponding half-times, $\tau_{1/2}$) for the labeling of Glu_{C4}, $GABA_{C2}$, Glu_{C3}, Asp_{C3} and Gln_{C4} (cortex only) were estimated by nonlinear least-squares fitting to a single exponential function (Fig. 2). A summary of analysis results appears in Table 1. With the exception of Asp_{C3} ($r^2 = 0.67$), a single exponential fit the data well with correlation coefficients of 0.89 to 0.97. The rate constant for Glu_{C4} turnover was significantly less for nerve terminals compared to homogenate ($P_{adj}=0.021$) or cortex ($P_{adj}<0.001$), corresponding to turnover times being longest in nerve terminals (21.8 min) compared to homogenate or cortex (12.4 to 14.2 min). The difference in the rate constant between homogenate and cortex was not significant ($P_{adj}>0.6$). For $GABA_{C2}$, the difference in turnover rate constant and half-times between terminals and cortex appeared slightly less marked than for Glu_{C4}, which did not reach statistical significance ($P=0.07$). Corresponding information for GABA (and glutamine) in the homogenate was not available, as these amino acids co-eluted with the highly concentrated sucrose in the neutral fraction, overwhelming their NMR signals and precluding their measurement. Differences in rate constants for Asp_{C3} turnover were not significant ($P_{adj}>0.8$). Averaging across homogenate and cortex, turnover times were longer for Asp_{C3} (~2.2x) and Glu_{C3} (~3.5x) compared to Glu_{C4}, consistent with the expected sequential delay in labeling of these carbon atom positions within the TCA cycle (Asp_{C3} is labeled in the 1st and 2nd turns, whereas Glu_{C3} is labeled in the 2nd turn), and the effect of label scrambling at fumarate C2 and C3.

Estimation of Glutamate and GABA Turnover Fluxes in Nerve Terminals and Tissues

The rate constants (Table 1) were used with estimates of total concentrations to calculate the turnover fluxes of Glu_{C4} and $GABA_{C2}$ in the terminals and tissue fractions. Total concentrations were determined only for cortex, which necessitated referencing glutamate and GABA to N-acetylaspartate (NAA)—a common endogenous marker of neurons with prominent signals in nerve terminals and cortex—for nerve terminals or assuming the values of concentrations outright for homogenate where NAA was not measured. We calculated average region-weighted brain concentrations for glutamate, GABA and NAA from data reported by Wang *et al.* [63] for forebrain (excludes olfactory bulb and cerebellum) and fronto-parietal cortex. While referencing nerve terminal concentrations to NAA avoids issues relating to possible variation in the efficiency of nerve terminal recovery from preparation to preparation, we have assumed that NAA concentration is the same (i.e., uniformly distributed) throughout neuronal cytoplasm, i.e., $[NAA]^{nt} = [NAA]^{hom}$. For the nerve terminals (nt) the Glu_{C4} and $GABA_{C2}$ turnover fluxes (F) were calculated as:

$$\mathrm{F}^{\mathrm{nt}}_{\mathrm{Glu4}} = k^{\mathrm{nt}}_{\mathrm{Glu4}} \times (\mathrm{Glu/NAA})^{\mathrm{nt}} \times ([\mathrm{NAA}]^{\mathrm{ctx}} \times f^{\mathrm{fb/ctx}}_{\mathrm{NAA}})$$
$$\mathrm{F}^{\mathrm{nt}}_{\mathrm{GABA2}} = k^{\mathrm{nt}}_{\mathrm{GABA2}} \times (\mathrm{GABA/NAA})^{\mathrm{nt}} \times ([\mathrm{NAA}]^{\mathrm{ctx}} \times f^{\mathrm{fb/ctx}}_{\mathrm{NAA}})$$

where the respective amino acid rate constants (k^{nt}_{AA}) and their ratios with NAA appear in Table 1, $[NAA]^{ctx}$ is the NAA concentration measured in cortex (10.2 ± 2.0 μmol·g^{-1}) and $f^{fb/ctx}_{NAA}$ (= 0.93) is the ratio of NAA in forebrain over fronto-parietal cortex calculated from brain regional concentrations and tissue weights reported in Table 1 and Supplement Table 2S, respectively, from [63]. For cortex (ctx) the Glu_{C4} and $GABA_{C2}$ turnover fluxes were calculated as

$$\mathrm{F}^{\mathrm{ctx}}_{\mathrm{Glu4}} = k^{\mathrm{ctx}}_{\mathrm{Glu4}} \times [\mathrm{Glu}]^{\mathrm{ctx}}$$
$$\mathrm{F}^{\mathrm{ctx}}_{\mathrm{GABA2}} = k^{\mathrm{ctx}}_{\mathrm{GABA2}} \times [\mathrm{GABA}]^{\mathrm{ctx}}$$

and similarly for homogenate:

$$\mathrm{F}^{\mathrm{hom}}_{\mathrm{Glu4}} = k^{\mathrm{hom}}_{\mathrm{Glu4}} \times ([\mathrm{Glu}]^{\mathrm{ctx}} \times f^{\mathrm{fb/ctx}}_{\mathrm{Glu}})$$

where the values for k^{ctx}_{Glu4}, k^{ctx}_{GABA2} and k^{hom}_{Glu4} appear in Table 1, while noting that GABA was not measured in the homogenate. The values of $[Glu]^{ctx}$ and $[GABA]^{ctx}$ are the respective glutamate (13.3 ± 1.2 μmol·g^{-1}) and GABA (2.5 ± 0.3 μmol·g^{-1}) concentrations measured in cortex, and $f^{fb/ctx}_{Glu}$ (= 0.93) and $f^{fb/ctx}_{Gaba}$ (= 1.29) are the respective ratios of forebrain over fronto-parietal cortex for glutamate and GABA calculated from Wang et al. [63].

Computing the turnover fluxes using these expressions and parameter estimates for Glu_{C4} gave 0.33 ± 0.09 μmol·g^{-1}·min^{-1} (nerve terminals), 0.60 ± 0.10 μmol·g^{-1}·min^{-1} (homogenate) and 0.74 ± 0.12 μmol·g^{-1}·min^{-1} (cortex). The corresponding $GABA_{C2}$

turnover fluxes were 0.16 ± 0.05 μmol·g^{-1}·min^{-1} (nerve terminals) and 0.12 ± 0.02 μmol·g^{-1}·min^{-1} (cortex).

Source of Steady-State Enrichment Dilution in Nerve Terminal Glutamate

To address whether inflow of an unlabeled substrate into the nerve terminals (e.g., glutamine) might explain the lower steady-state ^{13}C enrichments, we compared the ^{13}C labeling of Glu_{C4} in nerve terminals isolated from rats infused with either [2-^{13}C]acetate or [1,6-$^{13}C_2$]glucose. Unlike glucose, which is metabolized mainly by neurons, acetate (and [2-^{13}C]acetate) is metabolized predominately by astrocytes [64, 65], leading to labeling of Gln_{C4} by astrocyte specific, glutamine synthetase [66]. Following Gln_{C4} release from astrocytes and uptake into neurons, glutaminase action converts Gln_{C4} to Glu_{C4}. Therefore, the enrichment of Gln_{C4} will exceed Glu_{C4} following an infusion of [2-^{13}C]acetate, whereas the reverse is observed with [1,6-$^{13}C_2$]glucose as substrate. The ^{13}C labeling of Glu_{C4} in nerve terminals and cerebral cortex and of Gln_{C4} in cerebral cortex following short-time infusions of [1,6-$^{13}C_2$]glucose or [2-^{13}C]acetate is shown in Fig. 3. The ^{13}C labeling of Glu_{C4} from [1,6-$^{13}C_2$]glucose was significantly less in nerve terminals compared to cerebral cortex (P=0.001). In contrast to the labeling from glucose, Glu_{C4} percentage enrichment from [2-^{13}C]acetate in the nerve terminals was similar to cerebral cortex, although too few acetate-infused rats were studied to assess statistical significance. When expressed as the ratio, ^{13}C labeling from acetate relative to glucose was twice as large in the nerve terminals (0.28) than in cerebral cortex (0.13). Together with the findings of a higher steady-state dilution in Glu_{C4} from ^{13}C-labeled glucose (Table 1), the higher acetate-to-glucose enrichment ratio in nerve terminals strongly suggests that glutamate repletion from glutamine is more concentrated in the nerve terminals.

Estimation of Metabolic Fluxes in Cortex with Metabolic Modeling

Anesthetics depress metabolism in a dose and time dependent manner. To interpret differences in Glu_{C4} and $GABA_{C2}$ turnover between nerve terminals and whole tissue, and compare it to fluxes determined in anesthetized and awake rats in previous ^{13}C MRS studies, absolute fluxes were determined for fronto-parietal cortex by metabolic mathematical modeling. The three-compartment metabolic model described in Patel et al [24] and Methods was fitted to the enrichment time courses of blood plasma $glucose_{C1,6}$ and fronto-parietal cortex $Glu_{C4,C3}$, $GABA_{C2,C3}$, Gln_{C4} and Asp_{C3} (Fig. 4), providing estimates of rates of the TCA cycles, glutamate/GABA-glutamine cycles, glutamine synthesis, and related dilutions in neuronal (glutamatergic and GABAergic) and astroglial compartments (Table 2). The best fit of the metabolic model yielded estimates of the TCA cycle rate for glutamatergic neurons (0.68 ± 0.07 μmol·g^{-1}·min^{-1}), GABAergic neurons (0.21 ± 0.03 μmol·g^{-1}·min^{-1}) and astrocytes (0.24 ± 0.09 μmol·g^{-1}·min^{-1}), with neuronal oxidative metabolism comprising ~79% of the total (neurons plus astrocytes). The glutamate-glutamine and GABA-glutamine cycling rates were 0.31 ± 0.03 and 0.13 ± 0.02 μmol·g^{-1}·min^{-1}, respectively. The estimated rates of astrocytic glutamine ($V_{dil(Gln)}$) and neuronal (glutamate plus GABA) dilution ($V_{dil(N)}$) were ~0.44 and ~0.25 μmol·g^{-1}·min^{-1}, respectively.

Certain rates were assumed and used as fixed values in the model, including the ratios, $V_{cyc}/V_{TCA(N)}$ and pyruvate carboxylase-to-glutamine synthesis rates, V_{pc}/V_{Gln}, and the α-ketoglutarate-glutamate exchange rate in astrocytes, $V_{x(A)}$. We evaluated the sensitivity of the determined fluxes to these fixed parameters by altering their values by a fixed percentage above and below their nominal values (Supplementary Material, Table S2). The largest effect of a change (±25% of nominal) in $V_{cyc}/V_{TCA(N)}$ was seen in the for the dilution fluxes in glutamatergic neurons and astrocytes ($V_{dil(Glu)}$, −28% to 34%; $V_{dil(A)}$, 66% to −78%) and glial TCA cycle flux ($V_{TCA(A)}$, 17% to −20%), whereas effects on neuronal TCA cycle fluxes ($V_{TCA(Glu)}$, −5% to 6%; $V_{TCA(GABA)}$, ±7%;), glutamine synthesis (V_{gln}, ±0.7%), or glutamine dilution ($V_{dil(Gln)}$, ±0.7%) were small. For changes (±25% of nominal) in V_{pc}/V_{Gln}, the largest effects were seen on $V_{dil(A)}$ (18% to −17%) and $V_{TCA(A)}$ (±10%), whereas effects on all other fluxes ranged from 2% to <6%. For changes in $V_{x(A)}$ of 0.1 to 10 times $V_{TCA(A)}$, effects on the fluxes were minimal (<2%).

Discussion

This study determined the isotopic turnover of glutamate and related amino acids in forebrain nerve terminals and whole tissue fractions (forebrain homogenate and fronto-parietal cortex) from anesthetized rats infused intravenously with ^{13}C-labeled glucose or acetate. We found that the rate of Glu_{C4} turnover—a reflection of TCA cycle activity—was slower in nerve terminals than in brain homogenate or cortex, whereas their rates of $GABA_{C2}$ turnover were similar. Furthermore, we found that the steady-state ^{13}C enrichment, which reflects the sum of all substrate inflows to Glu_{C4} (both directly and indirectly through acetyl-CoA) was lower in nerve terminals compared to those in the tissue fractions—implying a dilution by non-isotopically labeled precursor substrate(s)—although this difference in enrichment (dilution) was less for $GABA_{C2}$. Employing [2-^{13}C]acetate, an astroglial substrate, we found the lower steady-state enrichment of Glu_{C4} from ^{13}C-glucose in the terminals is consistent with higher relative inflow of an unlabeled (or less C4 enriched) substrate, most likely glutamine [7, 26, 67–71].

The finding of a lower glutamate ^{13}C turnover rate in nerve terminals compared to that in the whole tissue was surprising, particularly as the metabolic rate at axon terminals/dendrites is believed to be the highest within a neuron based on studies using 2-deoxyglucose autoradiography in awake rats [72, 73]. This result may partly reflect the terminals being harvested from the whole forebrain, which includes many subcortical regions with metabolic rates lower than those seen in the cerebral cortex [38, 63, 74]. Indeed higher GABA/glutamate ratio was seen in the terminals (47%) compared to the cerebral cortex (19%), suggesting a somewhat different neuronal composition. However, the rate constant for Glu_{C4} turnover for forebrain homogenate, from which the nerve terminals were derived, was not significantly different from cortex (P_{adj}>0.6), indicating that other factors are more likely to explain the lower turnover rate observed. In our study, animals were anesthetized with halothane throughout the ^{13}C-glucose infusion and euthanasia, which would reduce cerebral metabolic fluxes relative to the awake state [74–77]. The TCA cycle and glutamate-glutamine cycle rates in glutamatergic neurons determined for the cortex by modeling of 0.68 μmol·g^{-1}·min^{-1} and 0.31 μmol·g^{-1}·min^{-1} (Table 2), were ~57–60% and ~54–69% of the corresponding rates (0.45–0.57 and 1.13–1.19 μmol·g^{-1}·min^{-1}) determined in awake rats

by Oz et al. [25]. Anesthesia alters activity-dependent glucose utilization associated with neural activity and neurotransmission [74, 78]. Therefore, halothane anesthesia may have had a greater effect in suppressing glucose oxidation in synaptic terminals/dendrites compared to the neuronal soma, effectively reducing ^{13}C enrichment and fluxes in nerve terminals relative to neuronal metabolic flux in the tissue as a whole. This can be seen quantitatively [27, 29] by considering the relationship between neurotransmitter glutamate-glutamine cycling and neuronal TCA cycle flux determined over a large range of neural activity (deep anesthesia to awake state) and described by the equation, $V_{TCA(n)} = 1.80V_{cyc} + 0.19$ [49]. This relation provides an estimate of the fraction of total neuronal TCA cycle flux (presynaptic terminals and dendrites, axons and soma) coupled to glutamate-glutamine cycling through the nerve terminals. For the anesthetized rats in our study, the fraction of glutamatergic TCA cycle flux associated with activity-dependent glutamate-glutamine cycling above the isoelectric (basal function) rate of 0.19 $\mu mol \cdot g^{-1} min^{-1}$ represents ~72% (= 100 x (0.68 – 0.19)/0.68) of the overall glutamatergic TCA cycle flux (Table 2). In awake rats, this fraction would be larger, ~83% (= 100 x (1.15 – 0.19)/1.15) assuming the same constant value of the basal rate. If the basal (non-glucose dependent) flux is higher, as suggested by some studies [49, 79], then the fraction of TCA cycle flux contributed by neurons (and their terminals) in response to neural activity would be correspondingly smaller. The findings that glutamate turnover flux in the nerve terminals was ~50% lower than homogenate or cortex is in-line with this overall interpretation.

The increased label dilution in Glu_{C4} in the nerve terminals compared to whole tissue homogenate or cerebral cortex was a significant finding. Differences in metabolic activity between regions or within cells (e.g., soma vs. axon terminals) contribute to the rate of ^{13}C turnover but not the steady-state enrichment, which reflects the sum of all the substrates (labeled and unlabeled) feeding the TCA cycles and glutamate pools. Aspartate-C3 also showed a high degree of ^{13}C label dilution in the terminals, similar to $Glu_{C4,}$ implying greater diluting inflow in this compartment. We found no evidence of an unlabeled metabolite(s) overlapping glutamate-H4 and aspartate-H3 to explain the lower enrichment.

The magnitude of the Glu_{C4} dilution seen in fronto-parietal cortex of 36% (= 100% - 64%; Table 1) is well within the range of 27–39% observed in cerebral cortex of rats infused with [1,6-$^{13}C_2$]glucose [39, 62]. Metabolic pathways that could potentially contribute to the isotopic label dilution in Glu_{C4} include blood-to-brain exchange with unlabeled lactate/pyruvate in blood [33], the pentose phosphate pathway (PPP) [80–83] and (or) dilution in Gln_{C4} transported to neurons via glutamine-to-glutamate cycling [28, 34, 70, 71]. Blood-to-brain lactate exchange is unlikely to be a major source of the Glu_{C4} dilution based on findings by Dienel et al. [83] of negligible exchange of brain lactate/pyruvate with blood following a brief pulse of ^{14}C-lactate. It is possible to estimate an upper limit of this dilution using the data reported in Herzog et al. [84]. In this study, [3-^{13}C]lactate was infused intravenously into anesthetized rats, raising blood lactate to ~3 mM (from ~1 mM basal) and ~35% ^{13}C enrichment. The infusion resulted in a time-dependent rise in Glu_{C4} enrichment to ~4% at isotopic steady state. Insulin was co-infused with lactate to suppress gluconeogenesis and ^{13}C label scrambling into glucose, ensuring that brain Glu_{C4} labeling arose directly from metabolism of ^{13}C-lactate. When normalized by the blood lactate enrichment (to 100%) and scaled downward to reflect physiological blood lactate levels (~1

mM), the predicted steady state Glu_{C4} enrichment (equivalent to dilution in the case of unlabeled blood lactate) would be ~3.8% (= (4%/35%) x (1mM/3mM)), which is ~$^1/_{10}$ of the observed dilution. As noted above, [1,6-$^{13}C_2$]glucose metabolized through the PPP, which results in the loss of C1 label as $^{13}CO_2$, reduces the enrichment at pyruvate-C3 relative to that produced solely by glycolysis. In neurons, pyruvate-C3 dilution arising through the PPP would not be distinguished in our experiment from the effects of blood-to-brain exchange of unlabeled lactate, whereas in the astrocytes either dilution would appear in the Gln_{C4} dilution. Estimates of PPP flux in brain range from 2–4% of total glucose metabolism [80–82], providing at most ~1–2% dilution of Glu_{C4} (50% loss of ^{13}C label due to metabolism of [1,6-$^{13}C_2$]glucose through the PPP). Thus, dilutions from blood lactate exchange and PPP together could account potentially for ~5–6% dilution of Glu_{C4}, or 14–17% of the total dilution observed. In modeling of the cortex enrichment time courses (Fig. 4), dilutions into α-ketoglutarate arising from lactate/pyruvate (V_{dil}) and into glutamine ($V_{dil(Gln)}$) were included as iterated fluxes. The relative contributions in neurons of the lactate/pyruvate and glutamine dilutions to overall dilution in Glu_{C4} can be approximated as the ratios, $V_{dil}/(V_{TCA}+V_{cyc})$ and $((V_{dil(Gln)}/V_{Gln}) \times V_{cyc})/(V_{TCA}+V_{cyc})$. Using values from Table 2 for glutamatergic neurons, estimates of the lactate/pyruvate and glutamine dilution fractions would be ~13% and ~25% of overall dilution, respectively. Thus, V_{dil} estimated by metabolic modeling for the cortex appears consistent with an estimate of combined lactate/pyruvate exchange and PPP. If V_{dil} and V_{TCA} scale proportionately in cortex and nerve terminals, the larger Glu_{C4} dilution in the nerve terminals of ~51% (= 100% – 48.5%; Table 1) can be attributed to increased flow from glutamine via glutamate-glutamine cycling.

Other sources of glutamate dilution in nerve terminals could come from glutamate trapped in vesicles that recycle very slowly (e.g., the reserve pool) or presynaptic reuptake of less-enriched glutamate from extracellular fluid. Estimates of the fraction of recycling vesicles in relation to total vesicles in nerve terminals of CNS synapses during physiological activity range from lows of 5–20% [85, 86] to most of all vesicles present [87]. Direct measurements of the ^{13}C enrichment of the vesicular glutamate in the nerve terminals will be required to resolve this issue. Pre-synaptic reuptake of glutamate into neurons has been shown [88] and nerve terminals express GLT-1 glutamate transporter [89]. Studies of mice with knockout of neuronal GLT-1 suggest that reuptake could account for up to 40% of synaptic clearance [89]. Considering the small extracellular diffusion volume of the synaptic cleft active zone (~44 x 10^{-3} μm^3 or <50 pL; [90]), the rapid turnover of this pool (e.g., cleft glutamate clearance in <20 msec at Calyx synapses [87]), and high glutamate-glutamine flux [29], the ^{13}C enrichment of cleft glutamate would be expected to follow closely the enrichment of released glutamate. Because the glutamate returning to the terminal by reuptake would have the same enrichment as vesicular glutamate, it is not likely to be the source of Glu_{C4} dilution.

We note that any label dilution in Glu_{C4} originating in neurons could not produce a level of dilution in Gln_{C4} exceeding that of Glu_{C4} at isotopic steady state, in general accord with the precursor-product relationship. The greater dilution seen in Gln_{C4} over that of Glu_{C4} at isotopic steady state (Table 1)[71] is related to metabolism of unlabeled substrates in astrocytes. This is seen experimentally in studies where [1,6-$^{13}C_2$]glucose is co-infused with unlabeled acetate (an astroglial precursor), resulting in significantly lower Glu_{C4} and Gln_{C4}

steady state enrichments [24] compared to [1,6-^{13}C]glucose infused alone [39]. The difference in labeling between Glu_{C4} and Gln_{C4} produced by the dilution in astrocytes was shown to be critically important for the determination and reliability of the glutamate/GABA-glutamine cycling rate in the ^{13}C MRS experiment [71].

The replenishment of glutamate in neurons by less enriched astroglial precursors during synaptic activity might be more prominent in the terminals [67]. The heightened enrichment of Glu_{C4} from ^{13}C-labeled acetate relative to glucose in nerve terminals, as compared to cerebral cortex, is consistent with an astroglial substrate(s), e.g. glutamine, as the likely source of isotopic dilution. In addition to glutamine, however, nerve terminals *in vitro* can also take up α-ketoglutarate, suggesting the potential for astroglial TCA cycle intermediates as precursors of neurotransmitter glutamate [56, 91], which would also possess a similar or higher dilution than glutamine. Glutamate formation from glutamine, however, is not limited to nerve terminals because mitochondrial phosphate-activated glutaminase (PAG) is present throughout the neuron [92], ensuring sufficient capacity for conversion of glutamine to glutamate. PAG inhibition by 6-diazo-5-oxo-L-norleucine leads to loss of glutamate in synaptosomes [93] and cell bodies of pyramidal (glutamatergic) neurons visualized *in situ* by immunostaining [94]. On the other hand, the concentrated release and regeneration of glutamate from glutamine in nerve terminals could lead to the higher constant dilution observed in this compartment, particularly if inducible glutamine transport and conversion of glutamine to glutamate is faster in the terminals during neural activity *in vivo* (e.g., see [95]).

In contrast to the lower average steady state enrichment (60+120 min) of Glu_{C4} in the nerve terminals, which differed from homogenate or cerebral cortex by ~18–24%, the difference in enrichment from cortex was less for $GABA_{C2}$ (~13%) (Table 1). This is not due to the absence of a diluting inflow in GABAergic terminals because $GABA_{C2}$ was less enriched than Glu_{C4} at steady-state (36.4% *vs.* 48.5%), indicating that GABA synthesis also involves a significant dilutional inflow. The smaller enrichment difference in $GABA_{C2}$ suggests that non-isotopic inflow (dilution) in glutamate precursors might occur more widely throughout the GABAergic neuron. Alternatively, the smaller physical size (and diffusion distance) of the majority of GABAergic neurons relative to glutamatergic neurons (e.g., pyramidal cells) would be anticipated to lead to faster mixing between nerve terminal and soma glutamate pools. Moreover, pioneering early studies [1, 2, 96] found that the glutamate precursor pool of GABA behaved kinetically as a physically compartmented smaller pool within the so-called ‘large pool glutamate’, both of which are present in the nerve terminals. Thus, the similar enrichment seen for $GABA_{C2}$ in cortex and nerve terminals, and for Gln_{C4} in cortex, along with the suspected low concentration of the glutamate precursor pool, suggests that in GABAergic neurons intracellular mixing of glutamate precursors used in GABA synthesis is more complete than in glutamatergic neurons. Further studies will be needed to confirm this possible mechanism.

The steady-state enrichment in $GABA_{C2}$ of 36–42% in terminals and cortex was less than the theoretical enrichment of 52% expected from the infused ^{13}C-labeled glucose acting as sole substrate, thus indicating that GABA synthesis also included a dilution flux component. This is consistent with previous descriptions of the glutamine dilution [70, 71] and

glutamine's contribution to GABA synthesis [5, 7, 14, 68, 69, 97–100]. Unlike synaptic release of glutamate, which is cleared mainly by astroglial glutamate transporters, GABA is extensively recycled after synaptic release by reuptake into GABAergic terminals via GABA transporters, as well as by astroglial uptake [4, 101, 102]. Because much of the basal GABA synthesis is mediated by GAD_{67} [103–105], which is expressed in the cytoplasm of cell bodies and terminals of GABAergic neurons, the reuptake/release of GABA by reversible GABA transporters might contribute to faster and more efficient mixing of GABA (labeled and unlabeled) between subcellular compartments.

In a previous study by Patel et al. [48], we reported that the rates of glucose phosphorylation in forebrain nerve terminals and tissue homogenate isolated *ex vivo* from halothane anesthetized rats infused with 2-fluorodeoxyglucose (FDG) were the same at rest and during seizures. The finding in the present study that the flux of glucose into nerve terminals was half that seen in homogenate or frontoparietal cortex (Table 1) suggests that under our study conditions, nerve terminals are more glycolytic, producing pyruvate in excess of oxidative needs. The question of whether neurons consume lactate provided by astrocytes [45, 106] or directly produce and release it [107] is unresolved. It should be possible in future studies to employ the nerve terminal preparation with prior co-infusions of FDG and ^{13}C-glucose to address this issue and others (e.g., the contribution of the PPP flux).

Limitations of the study

Methodological constraints limited our amino acid assessments in homogenates to glutamate and aspartate. In contrast to the extracts of fronto-parietal cortex, which did not contain the sucrose used to prepare the homogenates, or nerve terminals where sucrose was removed in the final step of their isolation, homogenate extracts contained high levels of sucrose. We used ion-exchange chromatography to separate sucrose from glutamate and aspartate, allowing fractional enrichments and their turnover to be determined, although no attempt was made to separate GABA and glutamine from co-eluted sucrose.

The animals in our study were anesthetized which may have affected the relationship between the measured fluxes as compared to the awake state. Anesthesia depresses glucose metabolism and glutamate-glutamine cycling proportionately above the isoelectric condition [27, 39, 46]. While this relationship has been determined for cerebral cortex, it has not been assessed for the nerve terminals. As discussed in Methods, anesthesia is assumed to alter metabolic rate (early times in the enrichment curve) but not the steady state enrichment, which reflects the inflows of all substrates (^{13}C labeled and unlableled) flowing into the glutamate pool. This assumes that the relative utilization of ^{13}C-labeled and unlabeled substrates in brain tissue and nerve terminals are not affected by anesthesia. In awake animals, we would expect Glu_{C4} enrichment to be higher in synaptic terminals (at early times during the ^{13}C-glucose infusion) compared to anesthetized animals, in line with what has been seen in anesthetized and awake rat cortex over a range of metabolic activity. This relationship, however, has not been assessed in nerve terminals and requires validation. The approach we have developed here should be valuable in this regard. Potential effects of anesthesia on the steady state ^{13}C enrichment are also possible, which could alter the relative label and dilutional flows to glutamate. Of the many studies performed under anesthesia,

reported values for the glutamine dilution (as measured by the difference between Glu_{C4} and Gln_{C4} over the blood glucose enrichment) appear similar, suggesting activity, per se, does not markedly alter this dilution. Further work is needed, however, to verify this in the nerve terminals under both low and high activity conditions, compartment where the magnitude of the glutamine dilution appears to be much greater.

The calculation of nerve terminal fluxes for glutamate and GABA were made by reference to N-acetylaspartate (NAA), a well-established neuron-specific marker [108], which we assumed to be constant in concentration throughout brain and neuronal cytoplasm. NAA synthesis occurs in mitochondria, and their presence/absence in different parts of a neuron might affect local NAA concentrations, leading to a potentially large source of error in the calculated fluxes. Mitochondria, however, are widely distributed throughout neurons, including the nerve terminals, and undergo continuous movement, as mitochondrial trafficking [109] plays an important role in matching energy supply to energy demand [110]. Nerve terminals prepared as in the current study, contain mitochondria along with numerous synaptic vesicles [48, 61]. The brain concentration of NAA in adult rats under physiologically normal conditions is relatively constant at ~6–8 mM across multiple brain regions [63]. A rough estimate of the diffusion time for NAA to travel a characteristic distance in the cell can be calculated using the Einstein-Smoluchowski relationship, which relates the diffusion coefficient (D, $\mu m^2 \cdot ms^{-1}$), displacement length (λ, μm) and time (τ, ms) as $\tau = \lambda^2/2D$. The apparent diffusion coefficient (D_{app}) of NAA in the brain as measured by MRS *in vivo* is ~0.27 $\mu m^2 \cdot ms^{-1}$ [111]. For a typical pyramidal neuron spanning ~2 mm of cortex, free diffusion would lead to complete mixing of NAA throughout the cytoplasm in about two hours (= $(2{,}000\ \mu m)^2/(2 \times (0.27\ \mu m^2 \cdot ms^{-1}) \times 1/3{,}600{,}000\ msec \cdot h^{-1})$). Compared to the several hours required for the slow turnover of NAA (time constant of 13–14 hours [112]), intracellular diffusion of NAA might be expected to minimize concentration differences throughout neuronal cytoplasm.

The *in vivo* NMR visibility of nerve terminal glutamate and other metabolites is currently unknown. In the present study we examined cell-free extracts where all components were NMR-visible and weighted mainly according to their concentration. To the extent that nerve terminal metabolites are partly or wholly NMR invisible *in vivo*, the concentration of glutamate and the contribution of the glutamine dilution to glutamate would be underestimated. Future studies using a diffusion-weighted NMR approach could conceivable resolve this issue.

The majority of studies modeling brain amino acid metabolism assumed that metabolic rates and labeling are constant within a given cell type, i.e., glutamatergic neurons, GABAergic neurons or astrocytes. Furthermore, it is assumed that within a neural cell all compartments have the same labeling, which would occur if diffusional mixing between compartments is relatively fast compared to the labeling rate within a compartment (e.g., nerve terminal, dendrite and soma) providing an accurate average rate of cellular metabolism. The present results suggest, however, that mixing between the nerve terminal and other compartments within glutamatergic neurons *in vivo* may not be fast enough to equalize labeling, at least under the conditions of anesthesia where metabolic rates are much slower. As a consequence of the increased dilution of the nerve terminal glutamate pool, the contribution of this

compartment to total cellular glutamate metabolism is likely to be underestimated in studies employing ^{13}C-labeled glucose. Future studies of nerve terminals isolated from single regions (e.g., from the cortex [100]) in awake animals should help to resolve this issue.

Conclusions

We have demonstrated that nerve terminals (synaptosomes) isolated *ex vivo* from rats receiving ^{13}C-labeled glucose or acetate by intravenous infusion provides unique information on the turnover of glutamate, GABA and other metabolites in the nerve terminal compartment as expressed *in vivo*. The ^{13}C isotopic turnover of nerve terminal amino acid pools displayed exponential kinetics, similar to that in whole tissue, thereby facilitating the application of metabolic modeling strategies. We found that Glu_{C4} turnover in nerve terminals was significantly slower than in whole tissue (forebrain homogenate or cortex), whereas $GABA_{C2}$ turnover was similar, findings which may be related to the effects of anesthesia and (or) differences in the rates of mixing of these pools with other glutamate containing pools. Nerve terminal glutamate-C4 also displayed a significantly higher dilution inflow coming from an unlabeled substrate. Nerve terminals isolated following infusion of [2-^{13}C]acetate, a glial substrate, showed a higher ratio of ^{13}C labeling in Glu_{C4} from [2-^{13}C]acetate over [1,6-^{13}C]glucose, suggesting that much of the dilution in Glu_{C4} isotopic enrichment arose from astroglial glutamine. This finding is consistent with the glutamate-glutamine cycle being the main source of repletion for nerve terminal glutamate. Future studies employing nerve terminals isolated from awake animals, and from more anatomically distinct brain regions, will undoubtedly resolve these mechanistic issues.

Supplementary Material

Refer to Web version on PubMed Central for supplementary material.

Acknowledgments

We thank Bei Wang for assistance with animal preparation and Terry Nixon, Peter Brown and Scott McIntire for the maintenance of the NMR spectrometer and related equipment in the Yale Magnetic Resonance Research Center. The assistance of Dr. Graeme Mason in the implementation of the Monte-Carlo fitting routines within the CWave software was greatly appreciated.

Funding: Support for this work came, in part, from grants by the National Institutes of Health, NIDDK R01-DK027121 and NINDS R01-NS34813.

References

1. van den Berg CJ, Garfinkel D. A stimulation study of brain compartments. Metabolism of glutamate and related substances in mouse brain. Biochem J. 1971; 123:211–218. [PubMed: 5164952]
2. Van den Berg CJ, Krzalic L, Mela P, Waelsch H. Compartmentation of glutamate metabolism in brain. Evidence for the existence of two different tricarboxylic acid cycles in brain. Biochem J. 1969; 113:281–290. [PubMed: 5808317]
3. Walls AB, Waagepetersen HS, Bak LK, Schousboe A, Sonnewald U. The glutamine-glutamate/GABA cycle: function, regional differences in glutamate and GABA production and effects of interference with GABA metabolism. Neurochem Res. 2015; 40:402–409. [PubMed: 25380696]
4. Schousboe A. Role of astrocytes in the maintenance and modulation of glutamatergic and GABAergic neurotransmission. Neurochem Res. 2003; 28:347–352. [PubMed: 12608708]

5. Erecinska M, Zaleska MM, Nissim I, Nelson D, Dagani F, Yudkoff M. Glucose and synaptosomal glutamate metabolism: studies with [^{15}N]glutamate. J Neurochem. 1988; 51:892–902. [PubMed: 2900879]
6. McKenna MC, Tildon JT, Stevenson JH, Hopkins IB. Energy metabolism in cortical synaptic terminals from weanling and mature rat brain: evidence for multiple compartments of tricarboxylic acid cycle activity. Dev Neurosci. 1994; 16:291–300. [PubMed: 7768208]
7. Yudkoff M, Zaleska MM, Nissim I, Nelson D, Erecinska M. Neuronal glutamine utilization: pathways of nitrogen transfer studied with [^{15}N]glutamine. J Neurochem. 1989; 53:632–640. [PubMed: 2746241]
8. McKenna MC. Glutamate pays its own way in astrocytes. Front Endocrinol (Lausanne). 2013; 4:191. [PubMed: 24379804]
9. McKenna MC. The glutamate-glutamine cycle is not stoichiometric: fates of glutamate in brain. J Neurosci Res. 2007; 85:3347–3358. [PubMed: 17847118]
10. Hertz L, Yu AC, Kala G, Schousboe A. Neuronal-astrocytic and cytosolic-mitochondrial metabolite trafficking during brain activation, hyperammonemia and energy deprivation. Neurochem Int. 2000; 37:83–102. [PubMed: 10812194]
11. Sonnewald U. Glutamate synthesis has to be matched by its degradation - where do all the carbons go? J Neurochem. 2014; 131:399–406. [PubMed: 24989463]
12. Badar-Goffer RS, Bachelard HS, Morris PG. Cerebral metabolism of acetate and glucose studied by 13C-n.m.r. spectroscopy. A technique for investigating metabolic compartmentation in the brain. Biochem J. 1990; 266:133–139. [PubMed: 1968742]
13. Sonnewald U, Westergaard N, Jones P, Taylor A, Bachelard HS, Schousboe A. Metabolism of [U-$^{13}C_5$] glutamine in cultured astrocytes studied by NMR spectroscopy: first evidence of astrocytic pyruvate recycling. J Neurochem. 1996; 67:2566–2572. [PubMed: 8931491]
14. Sonnewald U, Westergaard N, Schousboe A, Svendsen JS, Unsgard G, Petersen SB. Direct demonstration by [^{13}C]NMR spectroscopy that glutamine from astrocytes is a precursor for GABA synthesis in neurons. Neurochem Int. 1993; 22:19–29. [PubMed: 8095170]
15. Kanamori K, Kondrat RW, Ross BD. ^{13}C enrichment of extracellular neurotransmitter glutamate in rat brain--combined mass spectrometry and NMR studies of neurotransmitter turnover and uptake into glia in vivo. Cell Mol Biol (Noisy-le-grand). 2003; 49:819–836. [PubMed: 14528919]
16. Waagepetersen HS, Sonnewald U, Larsson OM, Schousboe A. Synthesis of vesicular GABA from glutamine involves TCA cycle metabolism in neocortical neurons. J Neurosci Res. 1999; 57:342–349. [PubMed: 10412025]
17. Waagepetersen HS, Sonnewald U, Larsson OM, Schousboe A. Multiple compartments with different metabolic characteristics are involved in biosynthesis of intracellular and released glutamine and citrate in astrocytes. Glia. 2001; 35:246–252. [PubMed: 11494415]
18. Waagepetersen HS, Sonnewald U, Schousboe A. Compartmentation of glutamine, glutamate, and GABA metabolism in neurons and astrocytes: functional implications. Neuroscientist. 2003; 9:398–403. [PubMed: 14580123]
19. Fitzpatrick SM, Hetherington HP, Behar KL, Shulman RG. The flux from glucose to glutamate in the rat brain *in vivo* as determined by ^{1}H-observed, ^{13}C-edited NMR spectroscopy. J Cereb Blood Flow Metab. 1990; 10:170–179. [PubMed: 1968068]
20. Cerdan S, Kunnecke B, Seelig J. Cerebral metabolism of [1,2-$^{13}C_2$]acetate as detected by in vivo and in vitro ^{13}C NMR. J Biol Chem. 1990; 265:12916–12926. [PubMed: 1973931]
21. Shen J, Sibson NR, Cline G, Behar KL, Rothman DL, Shulman RG. ^{15}N-NMR spectroscopy studies of ammonia transport and glutamine synthesis in the hyperammonemic rat brain. Dev Neurosci. 1998; 20:434–443. [PubMed: 9778582]
22. Gruetter R, Novotny EJ, Boulware SD, Mason GF, Rothman DL, Shulman GI, Prichard JW, Shulman RG. Localized ^{13}C NMR spectroscopy in the human brain of amino acid labeling from D-[1-^{13}C]glucose. J Neurochem. 1994; 63:1377–1385. [PubMed: 7931289]
23. Gruetter R, Seaquist ER, Ugurbil K. A mathematical model of compartmentalized neurotransmitter metabolism in the human brain. Am J Physiol Endocrinol Metab. 2001; 281:E100–112. [PubMed: 11404227]

24. Patel AB, de Graaf RA, Mason GF, Rothman DL, Shulman RG, Behar KL. The contribution of GABA to glutamate/glutamine cycling and energy metabolism in the rat cortex in vivo. Proc Natl Acad Sci U S A. 2005; 102:5588–5593. [PubMed: 15809416]
25. Oz G, Berkich DA, Henry PG, Xu Y, LaNoue K, Hutson SM, Gruetter R. Neuroglial metabolism in the awake rat brain: CO_2 fixation increases with brain activity. J Neurosci. 2004; 24:11273–11279. [PubMed: 15601933]
26. Sibson NR, Dhankhar A, Mason GF, Behar KL, Rothman DL, Shulman RG. In vivo ^{13}C NMR measurements of cerebral glutamine synthesis as evidence for glutamate-glutamine cycling. Proc Natl Acad Sci U S A. 1997; 94:2699–2704. [PubMed: 9122259]
27. Sibson NR, Dhankhar A, Mason GF, Rothman DL, Behar KL, Shulman RG. Stoichiometric coupling of brain glucose metabolism and glutamatergic neuronal activity. Proc Natl Acad Sci U S A. 1998; 95:316–321. [PubMed: 9419373]
28. Shen J, Petersen KF, Behar KL, Brown P, Nixon TW, Mason GF, Petroff OA, Shulman GI, Shulman RG, Rothman DL. Determination of the rate of the glutamate/glutamine cycle in the human brain by *in vivo* ^{13}C NMR. Proc Natl Acad Sci U S A. 1999; 96:8235–8240. [PubMed: 10393978]
29. Rothman DL, De Feyter HM, de Graaf RA, Mason GF, Behar KL. ^{13}C MRS studies of neuroenergetics and neurotransmitter cycling in humans. NMR Biomed. 2011; 24:943–957. [PubMed: 21882281]
30. Bluml S, Moreno A, Hwang JH, Ross BD. 1-^{13}C glucose magnetic resonance spectroscopy of pediatric and adult brain disorders. NMR Biomed. 2001; 14:19–32. [PubMed: 11252037]
31. Mason GF, Gruetter R, Rothman DL, Behar KL, Shulman RG, Novotny EJ. Simultaneous determination of the rates of the TCA cycle, glucose utilization, alpha-ketoglutarate/glutamate exchange, and glutamine synthesis in human brain by NMR. J Cereb Blood Flow Metab. 1995; 15:12–25. [PubMed: 7798329]
32. Mason GF, Rothman DL. Basic principles of metabolic modeling of NMR ^{13}C isotopic turnover to determine rates of brain metabolism in vivo. Metabol Eng. 2004; 6:75–84.
33. Mason GF, Rothman DL, Behar KL, Shulman RG. NMR determination of the TCA cycle rate and alpha-ketoglutarate/glutamate exchange rate in rat brain. J Cereb Blood Flow Metab. 1992; 12:434–447. [PubMed: 1349022]
34. Sibson NR, Mason GF, Shen J, Cline GW, Herskovits AZ, Wall JE, Behar KL, Rothman DL, Shulman RG. In vivo ^{13}C NMR measurement of neurotransmitter glutamate cycling, anaplerosis and TCA cycle flux in rat brain during [2-^{13}C]glucose infusion. J Neurochem. 2001; 76:975–989. [PubMed: 11181817]
35. Duarte JM, Gruetter R. Glutamatergic and GABAergic energy metabolism measured in the rat brain by ^{13}C NMR spectroscopy at 14.1 T. J Neurochem. 2013; 126:579–590. [PubMed: 23745684]
36. Choi IY, Lei H, Gruetter R. Effect of deep pentobarbital anesthesia on neurotransmitter metabolism *in vivo*: on the correlation of total glucose consumption with glutamatergic action. J Cereb Blood Flow Metab. 2002; 22:1343–1351. [PubMed: 12439292]
37. Henry PG, Lebon V, Vaufrey F, Brouillet E, Hantraye P, Bloch G. Decreased TCA cycle rate in the rat brain after acute 3-NP treatment measured by in vivo ^{1}H-[^{13}C]-NMR spectroscopy. J Neurochem. 2002; 82:857–866. [PubMed: 12358791]
38. de Graaf RA, Mason GF, Patel AB, Rothman DL, Behar KL. Regional glucose metabolism and glutamatergic neurotransmission in rat brain in vivo. Proc Natl Acad Sci U S A. 2004; 101:12700–12705. [PubMed: 15310848]
39. Patel AB, de Graaf RA, Mason GF, Kanamatsu T, Rothman DL, Shulman RG, Behar KL. Glutamatergic neurotransmission and neuronal glucose oxidation are coupled during intense neuronal activation. J Cereb Blood Flow Metab. 2004; 24:972–985. [PubMed: 15356418]
40. Lebon V, Petersen KF, Cline GW, Shen J, Mason GF, Dufour S, Behar KL, Shulman GI, Rothman DL. Astroglial contribution to brain energy metabolism in humans revealed by ^{13}C nuclear magnetic resonance spectroscopy: elucidation of the dominant pathway for neurotransmitter glutamate repletion and measurement of astrocytic oxidative metabolism. J Neurosci. 2002; 22:1523–1531. [PubMed: 11880482]

41. Hyder F, Fulbright RK, Shulman RG, Rothman DL. Glutamatergic function in the resting awake human brain is supported by uniformly high oxidative energy. J Cereb Blood Flow Metab. 2013; 33:339–347. [PubMed: 23299240]
42. Attwell D, Laughlin SB. An energy budget for signaling in the grey matter of the brain. J Cereb Blood Flow Metab. 2001; 21:1133–1145. [PubMed: 11598490]
43. Hyder F, Rothman DL, Bennett MR. Cortical energy demands of signaling and nonsignaling components in brain are conserved across mammalian species and activity levels. Proc Natl Acad Sci U S A. 2013; 110:3549–3554. [PubMed: 23319606]
44. Magistretti PJ, Pellerin L, Rothman DL, Shulman RG. Energy on demand. Science. 1999; 283:496–497. [PubMed: 9988650]
45. Pellerin L, Magistretti PJ. Glutamate uptake into astrocytes stimulates aerobic glycolysis: a mechanism coupling neuronal activity to glucose utilization. Proc Natl Acad Sci U S A. 1994; 91:10625–10629. [PubMed: 7938003]
46. Hyder F, Patel AB, Gjedde A, Rothman DL, Behar KL, Shulman RG. Neuronal-glial glucose oxidation and glutamatergic-GABAergic function. J Cereb Blood Flow Metab. 2006; 26:865–877. [PubMed: 16407855]
47. Occhipinti R, Somersalo E, Calvetti D. Astrocytes as the glucose shunt for glutamatergic neurons at high activity: an in silico study. J Neurophysiol. 2009; 101:2528–2538. [PubMed: 18922953]
48. Patel AB, Lai JC, Chowdhury GM, Hyder F, Rothman DL, Shulman RG, Behar KL. Direct evidence for activity-dependent glucose phosphorylation in neurons with implications for the astrocyte-to-neuron lactate shuttle. Proc Natl Acad Sci U S A. 2014; 111:5385–5390. [PubMed: 24706914]
49. Chowdhury GM, Jiang L, Rothman DL, Behar KL. The contribution of ketone bodies to basal and activity-dependent neuronal oxidation in vivo. J Cereb Blood Flow Metab. 2014
50. Caesar K, Hashemi P, Douhou A, Bonvento G, Boutelle MG, Walls AB, Lauritzen M. Glutamate receptor-dependent increments in lactate, glucose and oxygen metabolism evoked in rat cerebellum in vivo. J Physiol. 2008; 586:1337–1349. [PubMed: 18187464]
51. Lauritzen KH, Morland C, Puchades M, Holm-Hansen S, Hagelin EM, Lauritzen F, Attramadal H, Storm-Mathisen J, Gjedde A, Bergersen LH. Lactate receptor sites link neurotransmission, neurovascular coupling, and brain energy metabolism. Cereb Cortex. 2014; 24:2784–2795. [PubMed: 23696276]
52. Hall CN, Klein-Flugge MC, Howarth C, Attwell D. Oxidative phosphorylation, not glycolysis, powers presynaptic and postsynaptic mechanisms underlying brain information processing. J Neurosci. 2012; 32:8940–8951. [PubMed: 22745494]
53. Howarth C, Gleeson P, Attwell D. Updated energy budgets for neural computation in the neocortex and cerebellum. J Cereb Blood Flow Metab. 2012; 32:1222–1232. [PubMed: 22434069]
54. McKenna MC, Tildon JT, Stevenson JH, Hopkins IB, Huang X, Couto R. Lactate transport by cortical synaptosomes from adult rat brain: characterization of kinetics and inhibitor specificity. Dev Neurosci. 1998; 20:300–309. [PubMed: 9778566]
55. O'Brien J, Kla KM, Hopkins IB, Malecki EA, McKenna MC. Kinetic parameters and lactate dehydrogenase isozyme activities support possible lactate utilization by neurons. Neurochem Res. 2007; 32:597–607. [PubMed: 17006762]
56. Shank RP, Baldy WJ, Ash CW. Glutamine and 2-oxoglutarate as metabolic precursors of the transmitter pools of glutamate and GABA: correlation of regional uptake by rat brain synaptosomes. Neurochem Res. 1989; 14:371–376. [PubMed: 2569675]
57. McKenna MC, Stevenson JH, Huang X, Hopkins IB. Differential distribution of the enzymes glutamate dehydrogenase and aspartate aminotransferase in cortical synaptic mitochondria contributes to metabolic compartmentation in cortical synaptic terminals. Neurochem Int. 2000; 37:229–241. [PubMed: 10812208]
58. McKenna MC, Stevenson JH, Huang X, Tildon JT, Zielke CL, Hopkins IB. Mitochondrial malic enzyme activity is much higher in mitochondria from cortical synaptic terminals compared with mitochondria from primary cultures of cortical neurons or cerebellar granule cells. Neurochem Int. 2000; 36:451–459. [PubMed: 10733013]

59. McKenna MC, Hopkins IB, Lindauer SL, Bamford P. Aspartate aminotransferase in synaptic and nonsynaptic mitochondria: differential effect of compounds that influence transient hetero-enzyme complex (metabolon) formation. Neurochem Int. 2006; 48:629–636. [PubMed: 16513215]
60. Bogen IL, Risa O, Haug KH, Sonnewald U, Fonnum F, Walaas SI. Distinct changes in neuronal and astrocytic amino acid neurotransmitter metabolism in mice with reduced numbers of synaptic vesicles. J Neurochem. 2008; 105:2524–2534. [PubMed: 18346203]
61. Lai, JCK., Clark, JB. Isolation and characterization of synaptic and nonsynaptic mitochondria from mammalian brain. Humana Press, Inc; Clifton, N.J: 1989.
62. de Graaf RA, Brown PB, Mason GF, Rothman DL, Behar KL. Detection of [1,6-$^{13}C_2$]-glucose metabolism in rat brain by *in vivo* ^{1}H-[^{13}C]-NMR spectroscopy. Magn Reson Med. 2003; 49:37–46. [PubMed: 12509818]
63. Wang J, Jiang L, Jiang Y, Ma X, Chowdhury GM, Mason GF. Regional metabolite levels and turnover in the awake rat brain under the influence of nicotine. J Neurochem. 2010; 113:1447–1458. [PubMed: 20345764]
64. Waniewski RA, Martin DL. Preferential utilization of acetate by astrocytes is attributable to transport. J Neurosci. 1998; 18:5225–5233. [PubMed: 9651205]
65. Leke R, Bak LK, Schousboe A, Waagepetersen HS. Demonstration of neuron-glia transfer of precursors for GABA biosynthesis in a co-culture system of dissociated mouse cerebral cortex. Neurochem Res. 2008; 33:2629–2635. [PubMed: 18709552]
66. Patel AB, de Graaf RA, Rothman DL, Behar KL, Mason GF. Evaluation of cerebral acetate transport and metabolic rates in the rat brain in vivo using ^{1}H-[^{13}C]-NMR. J Cereb Blood Flow Metab. 2010; 30:1200–1213. [PubMed: 20125180]
67. Bradford HF, Ward HK, Thomas AJ. Glutamine--a major substrate for nerve endings. J Neurochem. 1978; 30:1453–1459. [PubMed: 670985]
68. Reubi JC, Van Der Berg C, Cuenod M. Glutamine as precursor for the GABA and glutamate trasmitter pools. Neurosci Lett. 1978; 10:171–174. [PubMed: 19605275]
69. Battaglioli G, Martin DL. Glutamine stimulates gamma-aminobutyric acid synthesis in synaptosomes but other putative astrocyte-to-neuron shuttle substrates do not. Neurosci Lett. 1996; 209:129–133. [PubMed: 8761999]
70. Dienel GA, Cruz NF. Exchange-mediated dilution of brain lactate specific activity: implications for the origin of glutamate dilution and the contributions of glutamine dilution and other pathways. J Neurochem. 2009; 109(Suppl 1):30–37. [PubMed: 19393006]
71. Shen J, Rothman DL, Behar KL, Xu S. Determination of the glutamate-glutamine cycling flux using two-compartment dynamic metabolic modeling is sensitive to astroglial dilution. J Cereb Blood Flow Metab. 2009; 29:108–118. [PubMed: 18766194]
72. Schwartz WJ, Smith CB, Davidsen L, Savaki H, Sokoloff L, Mata M, Fink DJ, Gainer H. Metabolic mapping of functional activity in the hypothalamo-neurohypophysial system of the rat. Science. 1979; 205:723–725. [PubMed: 462184]
73. Sokoloff, L. Brain Energetics and Neural Activity. John Wiley & Sons, Ltd; West Sussex, England: 2005. Energy metabolism in neural tissues in vivo at rest and in functionally altered states; p. 11-30.
74. Sokoloff L, Reivich M, Kennedy C, Des Rosiers MH, Patlak CS, Pettigrew KD, Sakurada O, Shinohara M. The [^{14}C]deoxyglucose method for the measurement of local cerebral glucose utilization: theory, procedure, and normal values in the conscious and anesthetized albino rat. J Neurochem. 1977; 28:897–916. [PubMed: 864466]
75. Kurumaji A, Nehls DG, Park CK, McCulloch J. Effects of NMDA antagonists, MK-801 and CPP, upon local cerebral glucose use. Brain Res. 1989; 496:268–284. [PubMed: 2553203]
76. Savaki HE, Desban M, Glowinski J, Besson MJ. Local cerebral glucose consumption in the rat. I. Effects of halothane anesthesia. J Comp Neurol. 1983; 213:36–45. [PubMed: 6826787]
77. Shapiro HM, Greenberg JH, Reivich M, Ashmead G, Sokoloff L. Local cerebral glucose uptake in awake and halothane-anesthetized primates. Anesthesiology. 1978; 48:97–103. [PubMed: 418710]
78. Savaki HE, Desban M, Glowinski J, Besson MJ. Local cerebral glucose consumption in the rat. II. Effects of unilateral substantia nigra stimulation in conscious and in halothane-anesthetized animals. J Comp Neurol. 1983; 213:46–65. [PubMed: 6826788]

79. Du F, Zhu XH, Zhang Y, Friedman M, Zhang N, Ugurbil K, Chen W. Tightly coupled brain activity and cerebral ATP metabolic rate. Proc Natl Acad Sci U S A. 2008; 105:6409–6414. [PubMed: 18443293]
80. Ben-Yoseph O, Camp DM, Robinson TE, Ross BD. Dynamic measurements of cerebral pentose phosphate pathway activity in vivo using [1,6-13C2,6,6-2H2]glucose and microdialysis. J Neurochem. 1995; 64:1336–1342. [PubMed: 7861166]
81. Gaitonde MK, Evison E, Evans GM. The rate of utilization of glucose via hexosemonophosphate shunt in brain. J Neurochem. 1983; 41:1253–1260. [PubMed: 6619864]
82. Hostetler KY, Landau BR. Estimation of the pentose cycle contribution to glucose metabolism in tissue in vivo. Biochem. 1967; 6:2961–2964. [PubMed: 6056970]
83. Dienel GA, Cruz NF, Nakanishi H, Melzer P, Moulis P, Sokoloff L. Comparison of rates of local cerebral glucose utilization determined with deoxy[1-^{14}C]glucose and deoxy[6-^{14}C]glucose. J Neurochem. 1992; 59:1430–1436. [PubMed: 1402893]
84. Herzog RI, Jiang L, Herman P, Zhao C, Sanganahalli BG, Mason GF, Hyder F, Rothman DL, Sherwin RS, Behar KL. Lactate preserves neuronal metabolism and function following antecedent recurrent hypoglycemia. J Clin Invest. 2013; 123:1988–1998. [PubMed: 23543056]
85. Denker A, Bethani I, Krohnert K, Korber C, Horstmann H, Wilhelm BG, Barysch SV, Kuner T, Neher E, Rizzoli SO. A small pool of vesicles maintains synaptic activity in vivo. Proc Natl Acad Sci U S A. 2011; 108:17177–17182. [PubMed: 21903928]
86. Harata N, Pyle JL, Aravanis AM, Mozhayeva M, Kavalali ET, Tsien RW. Limited numbers of recycling vesicles in small CNS nerve terminals: implications for neural signaling and vesicular cycling. Trends Neurosci. 2001; 24:637–643. [PubMed: 11672807]
87. Xue L, Sheng J, Wu XS, Wu W, Luo F, Shin W, Chiang HC, Wu LG. Most vesicles in a central nerve terminal participate in recycling. J Neurosci. 2013; 33:8820–8826. [PubMed: 23678124]
88. Waagepetersen HS, Qu H, Sonnewald U, Shimamoto K, Schousboe A. Role of glutamine and neuronal glutamate uptake in glutamate homeostasis and synthesis during vesicular release in cultured glutamatergic neurons. Neurochem Int. 2005; 47:92–102. [PubMed: 15921825]
89. Rimmele TS, Rosenberg PA. GLT-1: The elusive presynaptic glutamate transporter. Neurochem Int. 2016; 98:19–28. [PubMed: 27129805]
90. Schikorski T, Stevens CF. Quantitative ultrastructural analysis of hippocampal excitatory synapses. J Neurosci. 1997; 17:5858–5867. [PubMed: 9221783]
91. Peng L, Hertz L, Huang R, Sonnewald U, Petersen SB, Westergaard N, Larsson O, Schousboe A. Utilization of glutamine and of TCA cycle constituents as precursors for transmitter glutamate and GABA. Dev Neurosci. 1993; 15:367–377. [PubMed: 7805591]
92. Laake JH, Takumi Y, Eidet J, Torgner IA, Roberg B, Kvamme E, Ottersen OP. Postembedding immunogold labelling reveals subcellular localization and pathway-specific enrichment of phosphate activated glutaminase in rat cerebellum. Neurosci. 1999; 88:1137–1151.
93. Bradford HF, Ward HK, Foley P. Glutaminase inhibition and the release of neurotransmitter glutamate from synaptosomes. Brain Res. 1989; 476:29–34. [PubMed: 2563333]
94. Conti F, Minelli A. Glutamate immunoreactivity in rat cerebral cortex is reversibly abolished by 6-diazo-5-oxo-L-norleucine (DON), an inhibitor of phosphate-activated glutaminase. J Histochem Cytochem. 1994; 42:717–726. [PubMed: 7910617]
95. Billups D, Marx MC, Mela I, Billups B. Inducible presynaptic glutamine transport supports glutamatergic transmission at the calyx of Held synapse. J Neurosci. 2013; 33:17429–17434. [PubMed: 24174676]
96. Patel AJ, Johnson AL, Balazs R. Metabolic compartmentation of glutamate associated with the formation of gamma-aminobutyrate. J Neurochem. 1974; 23:1271–1279. [PubMed: 4156053]
97. Battaglioli G, Martin DL. Stimulation of synaptosomal gamma-aminobutyric acid synthesis by glutamate and glutamine. J Neurochem. 1990; 54:1179–1187. [PubMed: 1968957]
98. Battaglioli G, Martin DL. GABA synthesis in brain slices is dependent on glutamine produced in astrocytes. Neurochem Res. 1991; 16:151–156. [PubMed: 1881516]
99. Patel AB, Rothman DL, Cline GW, Behar KL. Glutamine is the major precursor for GABA synthesis in rat neocortex in vivo following acute GABA-transaminase inhibition. Brain Res. 2001; 919:207–220. [PubMed: 11701133]

100. Sonnewald U, McKenna M. Metabolic compartmentation in cortical synaptosomes: influence of glucose and preferential incorporation of endogenous glutamate into GABA. Neurochem Res. 2002; 27:43–50. [PubMed: 11926275]
101. Larsson OM, Hertz L, Schousboe A. Uptake of GABA and nipecotic acid in astrocytes and neurons in primary cultures: changes in the sodium coupling ratio during differentiation. J Neurosci Res. 1986; 16:699–708. [PubMed: 3025461]
102. Scimemi A. Structure, function, and plasticity of GABA transporters. Front Cell Neurosci. 2014; 8:161. [PubMed: 24987330]
103. Manor D, Rothman DL, Mason GF, Hyder F, Petroff OA, Behar KL. The rate of turnover of cortical GABA from [1-^{13}C]glucose is reduced in rats treated with the GABA-transaminase inhibitor vigabatrin (gamma-vinyl GABA). Neurochem Res. 1996; 21:1031–1041. [PubMed: 8897466]
104. Mason GF, Martin DL, Martin SB, Manor D, Sibson NR, Patel A, Rothman DL, Behar KL. Decrease in GABA synthesis rate in rat cortex following GABA-transaminase inhibition correlates with the decrease in GAD(67) protein. Brain Res. 2001; 914:81–91. [PubMed: 11578600]
105. Asada H, Kawamura Y, Maruyama K, Kume H, Ding RG, Kanbara N, Kuzume H, Sanbo M, Yagi T, Obata K. Cleft palate and decreased brain gamma-aminobutyric acid in mice lacking the 67-kDa isoform of glutamic acid decarboxylase. Proc Natl Acad Sci U S A. 1997; 94:6496–6499. [PubMed: 9177246]
106. Pellerin L, Magistretti PJ. Sweet sixteen for ANLS. J Cereb Blood Flow Metab. 2012; 32:1152–1166. [PubMed: 22027938]
107. Mangia S, Simpson IA, Vannucci SJ, Carruthers A. The in vivo neuron-to-astrocyte lactate shuttle in human brain: evidence from modeling of measured lactate levels during visual stimulation. J Neurochem. 2009; 109(Suppl 1):55–62. [PubMed: 19393009]
108. Moffett JR, Ross B, Arun P, Madhavarao CN, Namboodiri AM. N-Acetylaspartate in the CNS: from neurodiagnostics to neurobiology. Prog Neurobiol. 2007; 81:89–131. [PubMed: 17275978]
109. Schwarz TL. Mitochondrial trafficking in neurons. Cold Spring Harb Perspect Biol. 2013; :5.doi: 10.1101/cshperspect.a011304
110. Pekkurnaz G, Trinidad JC, Wang X, Kong D, Schwarz TL. Glucose regulates mitochondrial motility via Milton modification by O-GlcNAc transferase. Cell. 2014; 158:54–68. [PubMed: 24995978]
111. Pfeuffer J, Tkac I, Gruetter R. Extracellular-intracellular distribution of glucose and lactate in the rat brain assessed noninvasively by diffusion-weighted ^{1}H nuclear magnetic resonance spectroscopy *in vivo*. J Cereb Blood Flow Metab. 2000; 20:736–746. [PubMed: 10779018]
112. Choi IY, Gruetter R. Dynamic or inert metabolism? Turnover of N-acetyl aspartate and glutathione from D-[1-^{13}C]glucose in the rat brain *in vivo*. J Neurochem. 2004; 91:778–787. [PubMed: 15525331]

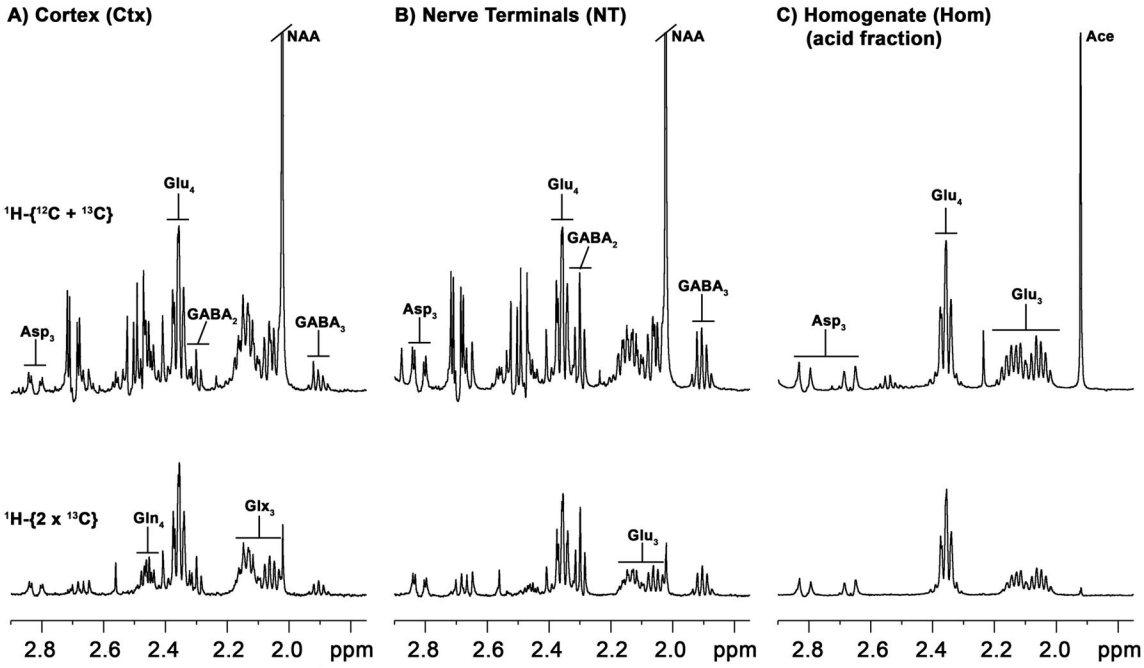

Fig. 1.

^{1}H-[^{13}C]-NMR spectra of extracted fronto-parietal cortex (a), forebrain nerve terminals (b), and forebrain homogenate separated by anion exchange chromatography (acid fraction) (c) from rats receiving intravenous [1,6-$^{13}C_2$]glucose for 2 hours. Upper spectra in A, B and C represent total proton intensity (bound to ^{13}C and ^{12}C), whereas lower spectra (^{1}H-[^{13}C] NMR difference spectrum) represent protons bound to ^{13}C atoms at twice the true intensity. Abbreviations: Asp, aspartate; GABA, γ-aminobutyric acid; Gln, glutamine; Glu, glutamate; Glx, glutamate + glutamine; NAA, N-acetylasparate; Ace, Acetate (acetate remaining after elution with 3M acetate and lyophilization). Numbered subscript refers to carbon atom position in the molecule.

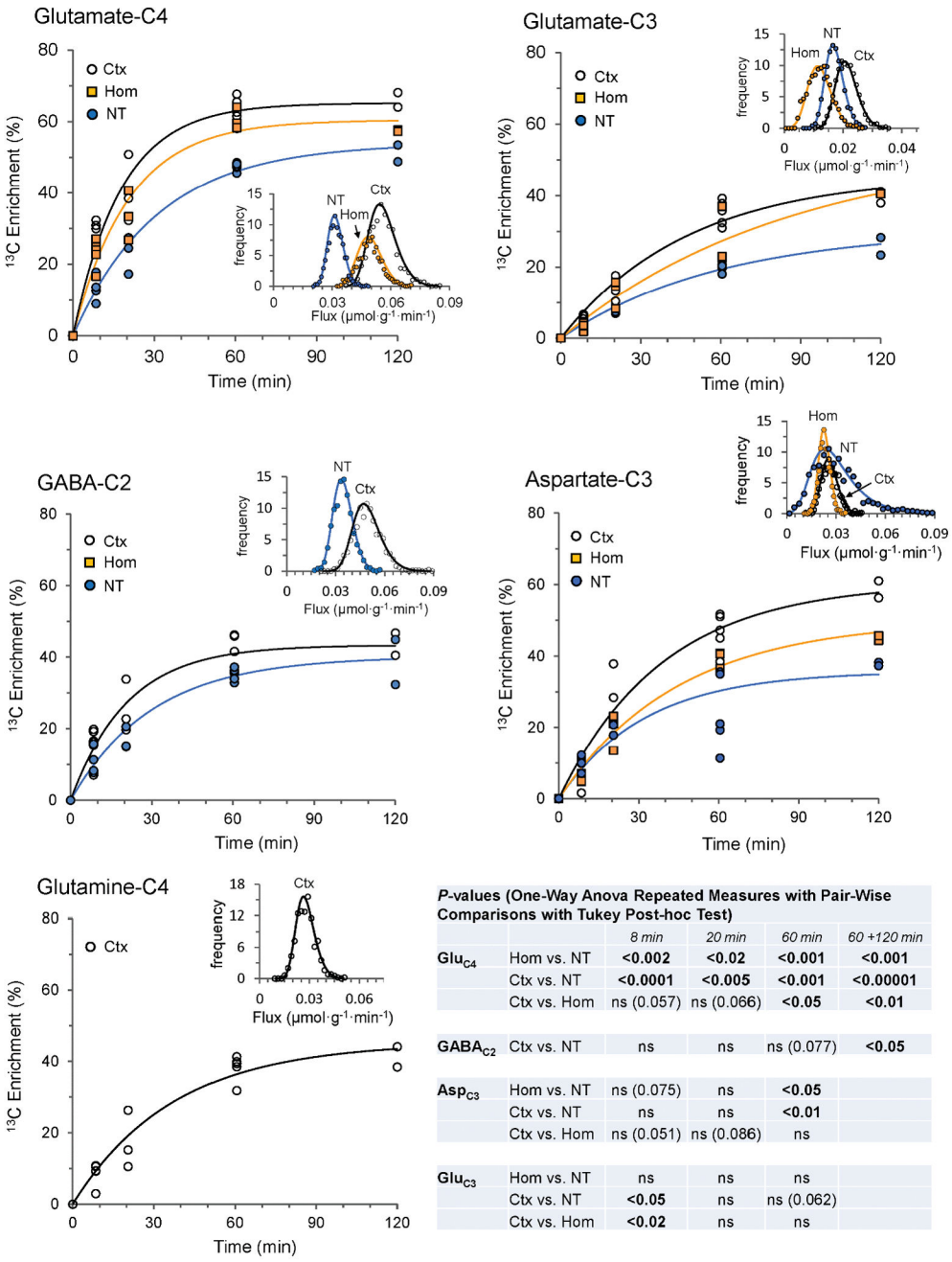

***P*-values (One-Way Anova Repeated Measures with Pair-Wise Comparisons with Tukey Post-hoc Test)**

		8 min	*20 min*	*60 min*	*60 +120 min*
Glu_{C4}	Hom vs. NT	**<0.002**	**<0.02**	**<0.001**	**<0.001**
	Ctx vs. NT	**<0.0001**	**<0.005**	**<0.001**	**<0.00001**
	Ctx vs. Hom	ns (0.057)	ns (0.066)	**<0.05**	**<0.01**
$GABA_{C2}$	Ctx vs. NT	ns	ns	ns (0.077)	**<0.05**
Asp_{C3}	Hom vs. NT	ns (0.075)	ns	**<0.05**	
	Ctx vs. NT	ns	ns	**<0.01**	
	Ctx vs. Hom	ns (0.051)	ns (0.086)	ns	
Glu_{C3}	Hom vs. NT	ns	ns	ns	
	Ctx vs. NT	**<0.05**	ns	ns (0.062)	
	Ctx vs. Hom	**<0.02**	ns	ns	

Fig. 2.

Ex vivo time courses of ^{13}C enrichment of amino acids in cerebral cortex (Ctx), homogenate (Hom) and nerve terminals (NT) in anesthetized rats receiving timed intravenous infusion of [1,6-$^{13}C_2$]glucose. Lines reflect best fit of a single exponential function to each data set consisting of 13-to-15 animals. Uncertainty distributions of the fitted rate constants (insets) for each turnover curve were assessed by Monte-Carlo simulation with 1000 iterations using the CWave software. P-values were determined from the distributions of the rate constants (see Table 1). Statistical significance of between-group differences in ^{13}C enrichments at the different time points was assessed by One-Way Repeated Measures ANOVA and Tukey's

Test. The 120 min time point consisted of too few animals (N=2) for statistical analysis and this data was combined (60 min + 120 min). The ^{13}C enrichment data from animals infused for 8 min and 60 minutes were taken from Patel *et al.* [48].

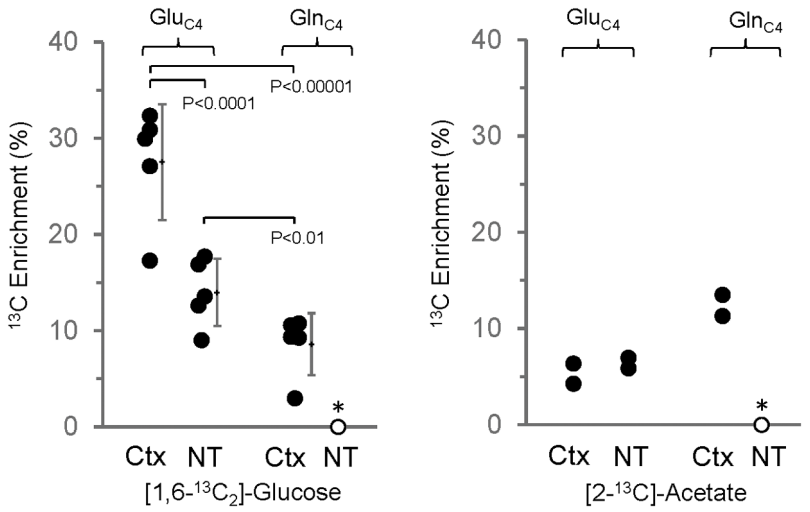

Fig. 3.

Comparison of ^{13}C enrichment of glutamate-C4 and glutamine-C4 in cerebral cortex (Ctx) and nerve terminals (NT) following intravenous infusion of either [1,6-$^{13}C_2$]glucose for 8 min (left panel, n=5) or [2-^{13}C]acetate for 15 min (right panel, n=2). For the glucose-infusion data, mean ± SD is shown to the right of each data set. Data points were separated slightly (horizontal scale) to improve clarity. P-values determined by One-Way ANOVA for Repeated Measures and Tukey's test. The symbols represent values of individual measurements. (*) Glutamine-C4 was below the level of detection in the nerve terminals.

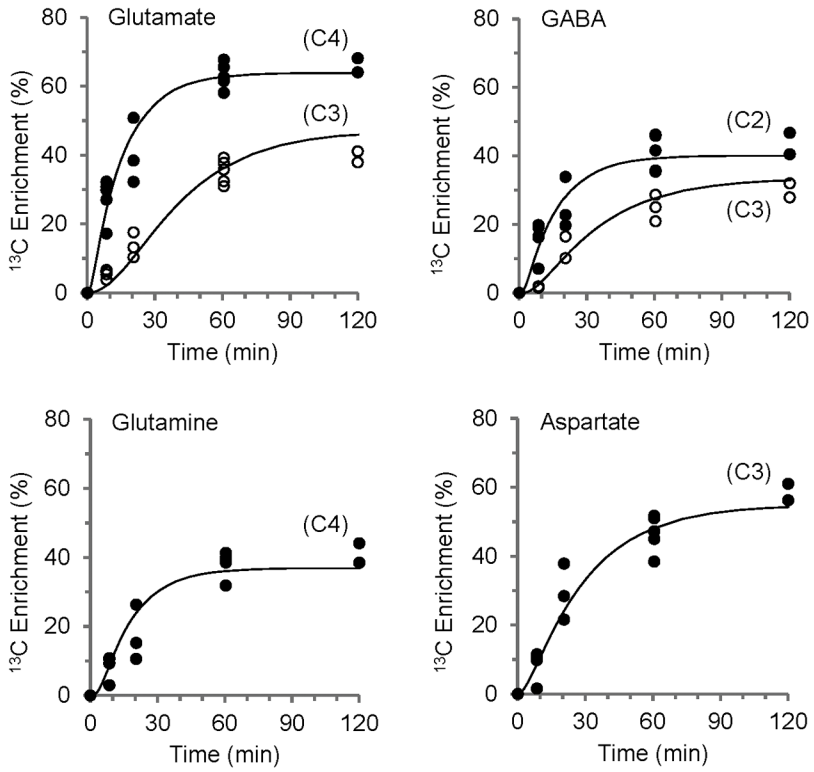

Fig. 4.

Fit of the metabolic model to the *ex vivo* time courses of amino acid labeling from [1,6-$^{13}C_2$]glucose for extracts of fronto-parietal cortex (Ctx). The line represents the best fit of a three-compartment (glutamatergic and GABAergic neurons, astrocytes) metabolic model to glutamate-C4 and -C3, GABA-C2 and –C3, glutamine-C4 and aspartate-C3 enrichment time courses, providing flux estimates for these neural cell populations in cerebral cortex (Table 2).

Neurochem Res. Author manuscript; available in PMC 2018 January 01.

Table 1

^{13}C Isotopic turnover kinetics and quasi-steady state enrichments of amino acids in forebrain nerve terminals and homogenate and cortical tissue from anesthetized rats infused intravenously with [1,6-$^{13}C_2$]glucose

		k **(min^{-1})**	**$\tau_{1/2}$ (min)**	**E_{SS}' (%)** [a]	**r^2**	**C_{tot}/NAA**	**C_{tot}** [b] **(μmol·g^{-1})**	**Flux** [f] **(μmol·g^{-1}·min^{-1})**
Glu_{C4}	NT	0.0318$^{*,\#\#}$ (0.0037)	21.8	48.5$^{***,\#\#\#}$ (2.4)	0.97	0.976 (0.138)	10.3[c] (2.6)	0.33 (0.09)
	Hom	0.0487 (0.0063)	14.2	59.4$^{\$}$ (2.8)	0.94		12.4[d] (1.4)	0.60 (0.10)
	Ctx	0.0559 (0.0071)	12.4	64.0 (3.6)	0.93		13.3[e] (1.2)	0.74 (0.08)
Glu_{C3}	NT	0.0168 (0.0030)	41.4		0.97			
	Hom	0.0116 (0.0041)	59.5		0.93			
	Ctx	0.0209 (0.0038)	33.1		0.96			
$GABA_{C2}$	NT	0.0330 (0.0059)	21.0	36.4 (4.3)	0.92	0.458 (0.061)	4.8[c] (1.2)	0.16 (0.05)
	Ctx	0.0477 (0.0084)	14.5	41.7 (4.8)	0.89		2.5[e] (0.29)	0.12 (0.02)
Gln_{C4}	Ctx	0.0268 (0.0054)	25.8	39.1 (3.7)	0.92		6.5 (0.74)	
Asp_{C3}	NT	0.0261 (0.0132)	26.5	28.3$^{*,\#\#}$ (11)	0.67	0.225 (0.092)	2.3[c] (0.94)	
	Hom	0.0224 (0.0035)	31.0	41.6 (3.6)	0.96		NA	
	Ctx	0.0257 (0.0050)	27.0	50.1 (7.4)	0.93		1.3[e] (0.51)	

Turnover parameters (mean (SE)) were estimated by non-linear least squares analysis of amino acid ^{13}C percentage enrichments *vs.* time data to a single exponential function using 12 to 15 rats per data set. Turnover half-times ($\tau_{1/2}$) were calculated as $\tau_{1/2} = ln(2)/k$.

P values for rate constant (*k*) group comparisons were estimated from the probability distributions calculated by Monte-Carlo analysis(see Fig. 2) and multiplied by 3 to adjust for comparisons between the three groups (NT, Hom, Ctx). P values for ESS′ group comparisons were determined by one-way ANOVA with repeated measures and Tukey's test to adjust for multiple comparisons. * P < 0.05, ** P < 0.001 and *** P < 0.0001 for comparisons of NT vs. Hom; # P < 0.05, $^{\#\#}$ P < 0.001 and $^{\#\#\#}$ P < 0.0001 for comparisons of NT vs. Ctx; $ P < 0.05 for comparisons of Hom vs. Ctx.

GluC4 glutamate-C4, *GluC3* glutamate-C3, *GABAC2* γ-aminobutyrate-C2, *GlnC4* glutamine-C4, *AspC3* aspartate-C3, *NT* nerve terminals, *Hom* homogenate, *Ctx* cortex, *NA* not available

[a] E_{SS}' is the apparent steady-state ^{13}C percentage enrichment averaged over 60 and 120 min (n = 5 to 7). Amino acid ^{13}C enrichments reflect excess above natural (1.1%) abundance, and were normalized by the respective animal's plasma glucose-C1 enrichment before computing group means. Equivalency of plasma glucose-C1 and -C6 ^{13}C enrichment was assumed.

[b] C_{tot} is the respective total (^{12}C+^{13}C) amino acid (AA) concentration (mean (SD)) as measured for cerebral cortex or estimated relative to N-acetylaspartate (NAA) in the nerve terminals.

[c] In nerve terminals, [NAA] was assumed to be equal to the average cortical concentration (11.32 ± 2.17 μmol·g^{-1}) multiplied by the forebrain-to-cortex ratio for NAA ($^{fb/ctx}NAA$ = 0.93) determined from Wang *et al.* [63].

[d] In homogenate, C_{tot} was calculated from the average cortical concentrations of glutamate (13.32 ± 1.22 μmol·g^{-1}) and GABA (2.50 ± 0.29 μmol·g^{-1}) multiplied by the respective forebrain-to-cortex ratio for glutamate ($f^{fb/ctx}_{Glu}$ = 0.93) or GABA ($f^{fb/ctx}_{Gaba}$ = 1.29) determined from Wang *et al.* [63]. NAA, which is present only in neurons, was assumed to be uniformly distributed in neuronal cytoplasm (see [48] for a discussion).

[e] In cortex, the respective amino acid concentrations (C_{tot}) were measured in the extract.

[f] Flux was calculated as the product, k x C_{tot}. The flux value for homogenate was determined using amino acid concentrations in cerebral cortex, and is considered an upper limit.

Definitions: Glu_{C4}, glutamate-C4; Glu_{C3}, glutamate-C3; $GABA_{C2}$, γ-aminobutyrate-C2; Gln_{C4}, glutamine-C4; Asp_{C3}, aspartate-C3; NT, Nerve Terminals; Hom, Homogenate; Ctx, Cortex; NA, not available; P-values for rate constant (k) group comparisons were estimated by t-test of the probability distributions calculated by Monte-Carlo analysis (see Fig. 2) and multiplied by 3 to adjust for comparisons between the three groups (NT, Hom, Ctx). P-values for E_{SS}' group comparisons were determined by one-way ANOVA with repeated measures and Tukey's test to adjust for multiple comparisons. * P<0.05, ** P<0.001 and *** P<0.0001 for comparisons of NT *vs.* Hom; # P<0.05, ## P<0.001 and ### P<0.0001 for comparisons of NT *vs.* Ctx; $ P<0.05 for comparisons of Hom *vs.* Ctx.

Table 2

Metabolic rates in cerebral cortical tissue estimated with the three-compartment model

	Metabolic Fluxes ($\mu molg^{-1}min^{-1}$)				
	V_{TCA}	V_{cyc}	V_{Gln}	V_{dil}	$V_{dil(Gln)}$
Glutamatergic neurons	0.68 (0.07)	0.31 (0.03)	—	0.13 (0.03)	—
GABAergic neurons	0.21 (0.03)	0.13 (0.02)	—	0.12 (0.02)	—
Astroglia	0.24 (0.09)	—	0.55 (0.04)	0.07 (0.05)	0.44 (0.09)

Values reflect best fits of a constrained three-compartment metabolic model as described in Methods to the ^{13}C percentage enrichment time courses of cerebral cortical tissue of halothane anesthetized rats. The rats were infused with [1,6-$^{13}C_2$]glucose for fixed infusion times and measured *ex vivo*. The fit reliability was improved by constraining the V_{cyc}/V_{TCAn} ratios for glutamatergic (0.45) and GABAergic (0.63) neuronal compartments to fixed values, determined in a previous study of halothane anesthetized rats in conjunction with a 2h infusion of [2-^{13}C]acetate [24]. Error estimates (in parentheses) reflect standard deviations for 1000 Monte-Carlo iterations. Definitions: V_{TCA}, TCA cycle rate; V_{cyc}, glutamate-glutamine or GABA-glutamine cycle rates, V_{Gln}, glutamine formation rate; V_{dil}, dilution rate in glutamatergic neurons, GABAergic neurons or astrocytes through lactate/pyruvate; $V_{dil(Gln)}$, glutamine dilution rate.